Integrative taxonomy of the gymnophthalmid lizard Neusticurus rudis Boulenger, 1900 identifies a new species in the eastern Pantepui region, north-eastern South America

Philippe J. R. Kok, Mátyás A. Bittenbinder, Joris K. van den Berg, Sergio Marques-Souza, Pedro M. Sales Nunes, Alexandra E. Laking, Mauro Teixeira Jr, Antoine Fouquet, D. Bruce Means, Ross D. MacCulloch & Miguel Trefaut Rodrigues

Published online: 09 Mar 2018.

Submit your article to this journal

View related articles

View Crossmark data

Taylor & Francis
Taylor & Francis Group

Check for updates

Integrative taxonomy of the gymnophthalmid lizard *Neusticurus rudis* Boulenger, 1900 identifies a new species in the eastern Pantepui region, north-eastern South America

Philippe J. R. Kok[a], Mátyás A. Bittenbinder[b], Joris K. van den Berg[b], Sergio Marques-Souza[c], Pedro M. Sales Nunes[d], Alexandra E. Laking[e], Mauro Teixeira Jr[c], Antoine Fouquet[f], D. Bruce Means[g], Ross D. MacCulloch[h] and Miguel Trefaut Rodrigues[c]

[a]Amphibian Evolution Lab, Biology Department, Vrije Universiteit Brussel, Brussel, Belgium; [b]Institute of Environmental Biology, Utrecht University, Utrecht, The Netherlands; [c]Laboratório de Herpetologia, Departamento de Zoologia, Instituto de Biociências, Universidade de São Paulo, São Paulo, Brazil; [d]Departamento de Zoologia, Centro de Biociências, Universidade Federal de Pernambuco, Recife, Brazil; [e]Department of Pathology, Bacteriology and Poultry disease, Faculty of Veterinary Medicine, Ghent University, Merelbeke, Belgium; [f]Laboratoire Écologie, Évolution, Interactions des Systèmes Amazoniens (LEEISA), USR 3456 (CNRS, IFREMER, Université de Guyane), Centre de Recherche de Montabo, Cayenne, French Guiana; [g]Coastal Plains Institute and Land Conservancy, Tallahassee, FL, USA; [h]Centre for Biodiversity and Conservation Biology, Royal Ontario Museum, Toronto, ON, Canada

ABSTRACT

The gymnophthalmid lizard genus *Neusticurus* Duméril and Bibron, 1839 currently contains six described species. One of them, *Neusticurus rudis* Boulenger, 1900 has a long history of taxonomic confusion, and uncertainty remains about the number of species involved under that name, especially in the Pantepui region. Our molecular phylogenetic (concatenation and species tree) and morphological (morphometrics, external and hemipenial morphology) analyses confirm *Neusticurus rudis* as a species complex with several candidate species in the eastern Pantepui region. *Neusticurus rudis* is here redescribed based on the re-examination of the holotype and 10 specimens from the vicinity of the type locality (ca. 15 km airline) in Guyana. The geographic distribution of *N. rudis* sensu stricto is restricted to east of the Venezuelan Gran Sabana, extending from the slopes of Mount Roraima in Venezuela through the slopes of Maringma-tepui and Wayalayeng to Mount Ayangganna in Guyana, between 678 and 1500 m elevation. Populations tentatively assigned to *N. rudis* also occur from Mount Wokomung in the Pakaraima Mountains of Guyana to the Iwokrama Forest Reserve in Guyana, between 159 and 1234 m elevation. A new *Neusticurus* species is described from the uplands and highlands of the eastern Pantepui region, west of the Venezuelan Gran Sabana in Brazil and Venezuela, between 900 and 2200 m elevation. Populations provisionally assigned to the new species were also found from the La Escalera region to Chivatón, the summit of Abakapá-tepui and the slopes and summit of Auyán-tepui, Venezuela, between 1100 and 2203 m elevation. Our results suggest the Gran Sabana as a possible recent biogeographical barrier for the genus in the region and indicate that tepui-summit *Neusticurus* populations derive from uplands populations that shifted their habitat preference.

www.zoobank.org/lsid:zoobank.org:pub:33DCF862-11CF-4FD0-B4D6-706E2C6A339E

**CONTACT** Philippe J. R. Kok ✉ philippe.kok@vub.be

Introduction

The family Gymnophthalmidae Fitzinger, 1826 currently comprises about 240 species distributed among ca. 47 genera (Uetz and Hosek 2017). Its taxonomy is in constant evolution with frequent erections of new subfamilies and genera, and generic reallocations of species (e.g. Kok 2015; Goicoechea et al. 2016; Torres-Carvajal et al. 2016; Sánchez-Pacheco et al. 2017; Marques-Souza et al. in press). Gymnophthalmids are endemic to the Neotropics and are ecologically and morphologically highly diverse, with some lineages predominantly found in semi-arid regions while some others are found in riparian habitats, such as the genus *Neusticurus* Duméril and Bibron, 1839. Molecular and morphological studies by Doan and Castoe (2005) indicated that the 11 species of *Neusticurus* known at that time fell in two statistically well-supported clades. A new genus, *Potamites* Doan and Castoe, 2005, was erected to accommodate species of one of these clades, while only five species remained in the genus *Neusticurus*: *Neusticurus bicarinatus* (Linnaeus, 1758), *Neusticurus medemi* Dixon and Lamar, 1981, *Neusticurus racenisi* Roze, 1958, *Neusticurus rudis* Boulenger, 1900 and *Neusticurus tatei* (Burt and Burt, 1931). *Neusticurus rudis* has a long history of taxonomic uncertainty, and the name *N. rudis* has possibly been assigned to several distinct 'cryptic' species (Donnelly and Myers 1991; Avila-Pires 1995; Barrio-Amorós and Brewer-Carías 2008; Rivas et al. 2012). Preliminary phylogenetic analyses (Kok et al. 2012) confirmed that *N. rudis* is indeed polyphyletic in the Guiana Shield. Recently, Marques-Souza et al. in press demonstrated that populations of *N. rudis* from the eastern Guiana Shield correspond to *Neusticurus surinamensis* Müller, 1923, raising the number of *Neusticurus* species to six. The existence of additional candidate species from Pantepui can be suspected from Kok et al. (2012). However, no additional conclusive evidence has been formally proposed for Pantepui populations of *N. rudis* yet, although this area, the 'Lost World' as coined by Doyle (1912), is of special interest. Pantepui (Figure 1) is a biogeographical region consisting of the remnants of a vast ancient sandstone plateau on the igneous-metamorphic basement of the Guiana Shield, where tepuis (sandstone table-top mountains) are the dominant landscape (see Kok 2013 for details). The origin and drivers of diversification of tepui-summit species/populations are still debated and several biogeographical hypotheses have been proposed (Mayr and Phelps 1967; see Kok 2013 for a summary). Recent phylogeographic studies (e.g. Kok et al. 2017, 2018b) highlighted the complexity of diversification patterns in the area.

Herein – based on specimens from 13 localities in Pantepui – we investigated the systematics of *Neusticurus rudis* in the eastern Pantepui region using molecular phylogenies based on concatenation and species tree analyses, and morphological evidence (morphometrics, hemipenial and external morphology). Based on these results we redescribe *Neusticurus rudis*, describe a related new species from the eastern Pantepui region, and reveal possible candidate species in this species complex.

Material and methods

Molecular data and laboratory procedure

We generated a total of 89 novel sequences for the nuclear oocyte maturation factor Mos gene (C-mos) and four mitochondrial markers, 16S ribosomal RNA gene (16S), 12S ribosomal RNA gene (12S), NADH dehydrogenase subunit four with flanking tRNA[His], tRNA[Ser] and
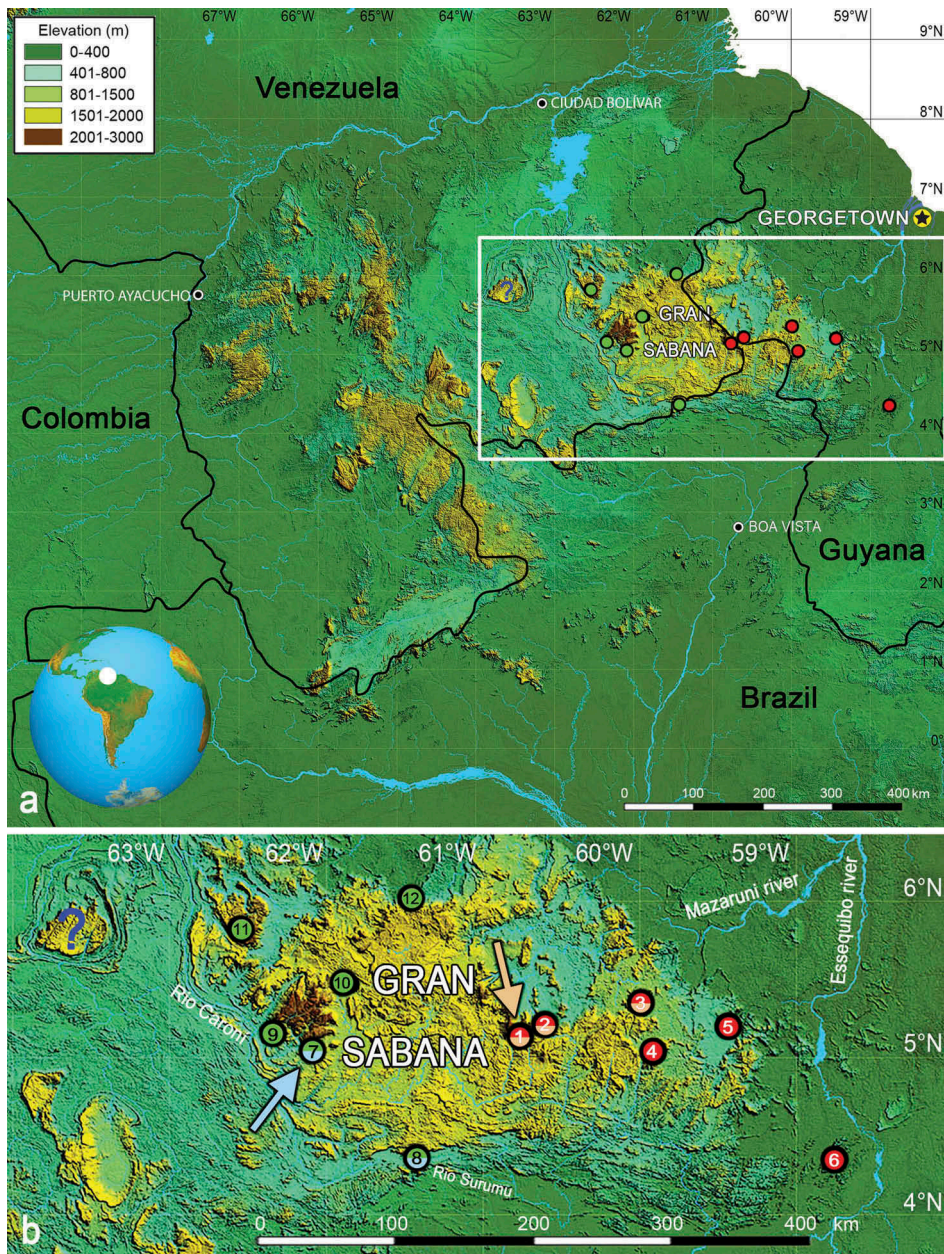
Figure 1. (a) Map of the Pantepui region showing the distributions of the *Neusticurus rudis* clade (red dots) and the *N. arekuna* clade (green dots). The white rectangle corresponds to the area enlarged in (b). (b) Distributions of the *Neusticurus rudis* clade (red dots) and the *N. arekuna* clade (green dots) with localities numbered as follows: (1) Mount Roraima, Venezuela/Guyana/Brazil (2) Maringma-tepui, Guyana; (3) Mount Ayanganna, Guyana; (4) Mount Wokomung, Guyana; (5) Kaieteur National Park, Guyana; (6) Iwokrama Mountains, Guyana; (7) Angasima-tepui, Venezuela; (8) Pacaraima, Brazil; (9) Abakapá-tepui, Venezuela; (10) Chivatón, Venezuela; (11) Auyán-tepui, Venezuela; (12) Salto El Danto/La Escalera, Venezuela. Coloured arrows highlight type localities of *N. rudis* (light brown) and *N. arekuna* sp. nov. (light blue). Circles whose bottom half is light brown depict the known localities of *N. rudis* sensu stricto; circles whose bottom half is light blue depict the known localities of *N. arekuna* sp. nov. sensu stricto. The blue question mark indicates an undetermined population from Guaiquinima-tepui, Venezuela (Donnelly and Myers 1991; Mägdefrau et al. 1991; Mägdefrau and Mägdefrau 1994; no specimen examined).

tRNA^{Leu} (ND4) and cytochrome b (cytb), from 27 specimens from 15 localities. These new sequences were combined with selected sequences from GenBank (Table 1). Total genomic DNA was isolated from tissue samples preserved in ethanol using the Qiagen DNeasy® Tissue Kit following the manufacturer's instructions. Gene fragments [ca. 525 base pairs (bp) of 16S, ca. 390 bp of 12S, ca. 880 bp of ND4, ca. 320 bp of cytb and ca. 390 bp of C-mos] were amplified using previously described primers, under previously described polymerase chain reaction (PCR) conditions (see Kocher et al. 1989; Arévalo et al. 1994; Palumbi 1996; Saint et al. 1998; Pellegrino et al. 2001; Godhino et al. 2006; Van Bocxlaer et al. 2010). PCR amplifications were confirmed on a 1% agarose gel, and sent to BaseClear BV (Leiden, The Netherlands) for subsequent purification and sequencing (along both strands using the same primers used for PCR). Chromatograms were read using CodonCode Aligner 5.0.2 (Codon Code Cooperation, Dedham, USA) and a consensus sequence was assembled from the forward and reverse primer sequences. Novel sequences have been catalogued in GenBank under the accession numbers MG906889–MG906977. MAFFT v7 (Katoh and Standley 2013) was used to perform preliminary sequences alignment using the G-INS-i algorithm and default parameters. Minor alignment corrections were made using MacClade 4.08 for Mac OS X (Maddison and Maddison 2005) and protein-coding genes were translated into amino-acid sequences to check for unexpected stop codons, which would be indicative of pseudogenes or misalignments. When present, ambiguous regions were excluded from subsequent analyses.

Molecular phylogenetic analyses

The combined 16S + 12S + ND4 + cytb + C-mos data set was subjected to phylogenetic inference using Bayesian analyses (Yang and Rannala 2012). The gymnophthalmid lizard genus *Proctoporus* Tschudi, 1845, was selected as the outgroup taxon. Optimal partitioning schemes were estimated with PartitionFinder v1.1.1 (Lanfear et al. 2012) using the 'greedy' algorithm, the 'mrbayes' set of models and the Bayesian information criterion (BIC) to compare the fit of different models. Bayesian posterior probabilities (PP) were used to estimate clade credibility in MrBayes 3.2.2 (Ronquist et al. 2012) on the CIPRES Science Gateway v3.3. The Bayesian analyses implemented the best substitution models inferred by PartitionFinder v1.1.1 partitioned over the different gene fragments, flat Dirichlet priors for base frequencies and substitution rate matrices and uniform priors for among-site rate parameters. Four parallel Markov chain Monte Carlo (MCMC) runs of four incrementally heated (temperature parameter = 0.2) chains were performed, with a length of 2.10^7 generations, a sampling frequency of 1 per 1000 generations, and a burn-in corresponding to the first 2.10^6 generations. Convergence of the parallel runs was confirmed by split frequency standard deviations (< 0.01) and potential scale reduction factors (~1.0) for all model parameters, as reported by MrBayes. All analyses were checked for convergence by plotting the log-likelihood values against generation time for each run, using Tracer 1.5 (Rambaut and Drummond 2009). All parameters had effective sample sizes (ESS) largely over 200.

In view of the results of the concatenated analysis (the population from Kaieteur National Park was shown to be polyphyletic), we additionally conducted a species tree analysis using a Bayesian multispecies coalescent approach implemented in *BEAST (BEAST 2.4.4 package; Drummond et al. 2012) based on the same loci used for the

Table 1. List of genetic samples used in this study, with localities and GenBank accession numbers. Sequences newly generated are in **boldface**; UCS = unconfirmed candidate species; NA = not available.

GenBank voucher	Taxon	Locality	Country	Coordinates	Elevation (m)	16S	12S	ND4	cytb	C-mos
IRSNB18146	*Neusticurus rudis sensu stricto*	Maringma-tepui	Guyana	5°12.6167N, 60°33.9833W	1060	JQ742244	**MG906902**	**MG906926**	NA	NA
IRSNB18147	*N. rudis* sensu stricto	Maringma-tepui	Guyana	5°12.2667N, 60°34.65W	1376	JQ742245	**MG906903**	NA	NA	**MG906957**
ROM39498	*N. rudis* sensu stricto	Mount Ayanganna	Guyana	5°21.1N, 59°57.4W	1490	JQ742248	**MG906904**	NA	NA	**MG906958**
IRSNB17344	*N. rudis* UCS 1	Kaieteur National Park	Guyana	5°8.7333N, 59°25.5167W	515	JQ742242	**MG906905**	**MG906927**	**MG906946**	**MG906959**
ROM42644	*N. rudis* UCS 1	Wokomung Massif	Guyana	5°6.5833N, 59°49.2667W	1234	JQ742249	**MG906906**	**MG906928**	**MG906947**	**MG906960**
IRSNB17345	*N. rudis* UCS 1	Kaieteur National Park	Guyana	5°8N, 59°24W	580	JQ742243	**MG906907**	NA	NA	NA
ROM20514	*N. rudis* UCS 1	Kaieteur National Park	Guyana	5°12N, 59°27W	205	JQ742247	**MG906908**	NA	NA	**MG906961**
IRSNB18440	*N. rudis* UCS 2	Iwokrama Forest	Guyana	4°19.8167N, 58°47.9W	195	**MG906889**	**MG906909**	**MG906929**	NA	**MG906962**
IRSNB18442	*N. rudis* UCS 2	Iwokrama Forest	Guyana	4°24.7667N, 58°47.0333W	159	**MG906890**	**MG906910**	**MG906930**	NA	NA
IRSNB18441	*N. rudis* UCS 2	Iwokrama Forest	Guyana	4°19.8167N, 58°47.9W	195	**MG906891**	NA	**MG906931**	NA	NA
IRSNB18443	*N. rudis* UCS 2	Iwokrama Forest	Guyana	4°24.7667N, 58°47.0333W	159	**MG906892**	NA	**MG906932**	NA	NA
IRSNB18151 (now IRSNB2688)	*N. arekuna* sensu stricto	Angasima-tepui	Venezuela	5°02.5833N, 62°04.8667W	2162	JQ742241	**MG906911**	**MG906933**	**MG906948**	**MG906963**
MZUSP106223	*N. arekuna* sensu stricto	Pacaraima	Brazil	4°27.6333N, 61°8.7W	900	**MG906893**	**MG906912**	**MG906934**	NA	**MG906964**
MZUSP106226	*N. arekuna* sensu stricto	Pacaraima	Brazil	4°27.6333N, 61°8.7W	900	**MG906894**	**MG906913**	**MG906935**	NA	**MG906965**
MZUSP106227	*N. arekuna* sensu stricto	Pacaraima	Brazil	4°27.6333N, 61°8.7W	900	**MG906895**	**MG906914**	**MG906936**	NA	**MG906966**
MZUSP106224	*N. arekuna* sensu stricto	Pacaraima	Brazil	4°27.6333N, 61°8.7W	900	**MG906896**	**MG906915**	**MG906937**	NA	**MG906967**
MZUSP106225	*N. arekuna* sensu stricto	Pacaraima	Brazil	4°27.6333N, 61°8.7W	900	**MG906897**	**MG906916**	**MG906938**	NA	**MG906968**
PK2058V	*N. arekuna* UCS 1	Chivatón	Venezuela	5°35.25N, 61°40.8333W	1400	JQ742246	**MG906917**	NA	**MG906949**	NA
IRSNB18150	*N. arekuna* UCS 1	Abakapá-tepui	Venezuela	5°11.1N, 62°17.4667W	2156	JQ742240	**MG906918**	**MG906939**	**MG906950**	**MG906969**
IRSNB18109	*N. arekuna* UCS 2	Salto El Danto	Venezuela	5°57.8667N, 61°23.5167W	1208	JQ742251	**MG906919**	**MG906940**	**MG906951**	**MG906970**
IRSNB18111	*N. arekuna* UCS 2	La Escalera	Venezuela	5°57N, 61°23W	1100	JQ742253	**MG906920**	**MG906941**	**MG906952**	**MG906971**
IRSNB18110	*N. arekuna* UCS 2	La Escalera	Venezuela	5°57N, 61°23W	1100	JQ742252	**MG906921**	NA	**MG906953**	**MG906972**
IRSNB18455	*N. arekuna* UCS 3	Auyán-tepui	Venezuela	5°45.6167N, 62°31.0333W	2203	**MG906898**	**MG906922**	**MG906942**	**MG906954**	**MG906973**
IRSNB18456	*N. arekuna* UCS 3	Auyán-tepui	Venezuela	5°45.6167N, 62°31.0333W	2203	**MG906899**	NA	NA	**MG906955**	**MG906974**
IRSNB18149	*N. surinamensis*	Kaw Mountain	French Guiana	4°32.6833N, 52°9.15W	211	JQ742250	**MG906923**	**MG906943**	**MG906956**	**MG906975**
MRT977116	*N. bicarinatus*	Juruena	Brazil	10°20.4S, 58°34.9W	NA	**MG906901**	**MG906924**	**MG906944**	NA	**MG906976**
MTR20743	*N. racenisi*	Pacaraima	Brazil	4°27.6333N, 61°8.7W	900	**MG906900**	**MG906925**	**MG906945**	NA	**MG906977**
CORBIDI8416	*Proctoporus chasqui*	La Mar	Peru	NA	NA	KU902246	KU902166	KU902323	NA	KU902085

concatenated analysis. Each terminal was assigned to a described species or to a morphologically distinct population. The following setting of priors was found to work best (i.e. avoiding overparameterisation) with our data set: we used a linked tree model for the mitochondrial genes, a strict clock, a Coalescent Constant Population speciation prior on tree shape, the HKY model for each locus, and the piecewise linear and constant root population size model; analyses were initiated with a random starting tree for each locus; the population mean was given a uniform prior and the population size a lognormal prior. Other parameters were left at their default values. The *BEAST analysis was run with a chain length of 1.10^8, and a 10% cut-off was used for the burn-in. The convergence was checked in Tracer 1.6.0 (Rambaut and Drummond 2007) with ESS ≥ 200. Resulting trees were summarised in LogCombiner 2.4.4 and TreeAnnotator 2.4.4 (part of the BEAST package). Results were visualised and edited in FigTree 1.4.3 (Rambaut 2016) and DensiTree (Bouckaert and Heled 2014).

We also calculated uncorrected p-distances in the 16S and ND4 mitochondrial genes among all the *Neusticurus* lineages recovered from the phylogenetic analysis using PAUP 4.0b150 (Swofford 2002).

Hemipenial morphology

In a few male specimens examined one or both hemipenes were everted in the field by the collector. The hemipenes of six individuals from different populations of *Neusticurus rudis* (Angasima-tepui, Venezuela [1], Pacaraima, Brazil [1]; Abakapá-tepui, Venezuela [1]; Maringma-tepui, Guyana [1]; and Iwokrama, Guyana [2]) were dissected in the laboratory, and prepared following the procedures described by Manzani and Abe (1988) and modified by Pesantes (1994) and Zaher (1999). The retractor muscle was manually separated and the everted organs filled with stained petroleum jelly. Organs were soaked in an alcoholic solution of Alizarin Red for 24 hours to stain possible calcified structures (e.g. spines or spicules), in an adaptation proposed by Nunes et al. (2012) of the procedures described by Uzzell (1973) and Harvey and Embert (2008). The terminology of hemipenial structures follows Dowling and Savage (1960), Savage (1997) and Myers and Donnelly (2001, 2008).

Morphometrics and external morphology

We examined high-resolution digital photographs of the holotype of *Neusticurus rudis* (BM1946.8.31.64, specimen currently missing in the Natural History Museum, London, D. Gower pers. comm. September 2014) as well as 73 museum specimens of *Neusticurus* species, originating from multiple localities in Venezuela, Guyana, Suriname, French Guiana and Brazil (see below, Table 2 and Appendix 1).

The following measurements were taken (by MAB, JKB and SMS) on the preserved specimens using digital callipers, rounded to 0.1 mm, and abbreviated as follows: (1) snout–vent length (SVL), from tip of snout to cloacal aperture; (2) head length (HL), from tip of snout to posterior margin of tympanum; (3) snout–collar length (SCL), from tip of snout to collar plate; (4) head width (HW), greatest width of head; (5) neck length (NL), from posterior margin of tympanum to forearm held at right angle to body (= anterior insertion of forelimb); (6) snout–axilla length (SAL), from tip of snout to anterior insertion of forelimb; (7) axilla–groin distance (AXG), from axilla to base of hindlimb (groin); (8) forelimb length (FiL), from axilla to tip of claw

of the 4th finger; (9) hindlimb length (HiL), from groin to tip of claw of the 4th toe; (10) tail length (TL), from posterior margin of vent to the tip of tail; (11) frontal length (FL) and frontonasal length (FnL). Body parts (e.g. limbs, tail) that were not measurable using callipers were measured with a piece of string and a ruler.

The following scales were counted and abbreviated as follows: (1) frontonasals (Fn); (2) supralabials (SL); (3) infralabials (IL); (4) genials (G); (5) palpebrals in translucent disc (P); (6) supraciliaries (SC); (7) supraoculars (SO); (8) suboculars (SuO); (9) total number of occipitals (O); (10) occipitals in contact with the posterior edge of parietals and interparietal (Oc); (11) collar scales (Co); (12) dorsal tubercles in a longitudinal row (Tu); (13) ventral scales in transverse rows between the collar and the preanal plate, counted along the median row (VT); (14) ventral scales in longitudinal rows, including the small ventrolateral scales (VL); (15) subdigital lamellae under the 4th finger, taken on the right hand, ungual sheath omitted (SLF); (16) subdigital lamellae under the 4th toe, taken on the right foot, ungual sheath omitted (SLT).

Additional features examined were: (17) sex, which was determined through a small incision along the ventrolateral part of the base of the tail to determine whether hemipenes were present (this was performed only when hemipenes were not previously everted in the field); (18) condition of the tympanum, where two conditions were considered: moderately or deeply recessed; (19) size, shape and position of scales on head (e. g. occipitals, temporals, gulars) as well as the condition and position of scales on nape, back and flanks; (20) condition of tail segments (verticils), and number of scale rows on each; (21) number and condition of cloacal scales on the preanal plate; and (22) total number of femoral pores (FP).

Colour pattern

Colour pattern in life and in preservative was determined using field notes, digital photographs of living specimens, and preserved specimens examined as well as pictures and descriptions provided in the literature (e.g. Burt and Burt 1931; Uzzell 1966; Hoogmoed 1973; Dixon and Lamar 1981; Donnelly and Myers 1991; Avila-Pires 1995; Barrio-Amorós and Brewer-Carías 2008).

Results

Molecular phylogenetic analyses

Bayesian analyses performed on the concatenated data set (2500 bp of aligned sequences) recovered a mostly well-supported phylogeny (Figure 2) – except for the position of *Neusticurus racenisi* recovered as sister to the clade containing *N. bicarinatus* and *N. surinamensis* with low support (PP = 0.58) – and showing a monophyletic *N. rudis* (PP = 1) with considerable genetic structure. Two main clades are recovered within *N. rudis*, geographically separated from each other by the Venezuelan Gran Sabana. The clade containing samples from west of the Gran Sabana (PP = 1, shown in green in Figure 2) contains two strongly supported clades: one poorly structured clade (PP = 1) containing samples from the summit of Angasima-tepui (Bolívar state, Venezuela) + samples from Pacaraima (Roraima state, Brazil); the other clade (PP = 1) is divided into two main subclades, one subclade

Table 2. Variation of selected morphological and meristic characters among populations of *Neusticurus rudis* and *N. arekuna* sensu lato. BM = Natural History Museum, London (United Kingdom); CPI = Coastal Plains Institute and Land Conservancy (USA); IRSNB = Institut Royal des Sciences Naturelles de Belgique (Belgium); MZUSP = Museu de Zoologia da Universidade de São Paulo (Brazil); UCS = unconfirmed candidate species; M = male; F = female; JUV = juvenile; other abbreviations are explained in the text.

Taxon	Museum voucher	Locality	Sex	SVL	TL	HL	HW	NL	AXG	FiL	HiL	Fn	Oc	VL	VT	SLF	SLT	FP	SL	IL	SO
Neusticurus rudis	BM1946.8.31.64	Mount Roraima	M	59.0	124.0	14.0	8.5	NA	NA	19.0	27.0	2	11	8	28	19	29	40	7	4	3
N. rudis	IRSNB18146	Maringma-tepui	M	76.2	136.9	17.7	12.0	11.4	35.6	29.9	46.6	2	10	8	25	19	29	40	7	4	3/4
N. rudis	IRSNB18147	Maringma-tepui	F	56.6	128.0	13.9	9.3	10.4	26.4	23.5	37.4	2	7	8	27	18	27	49	7	4	4
N. rudis	IRSNB18431	Wayalayeng	JUV	32.3	59.3	7.9	5.2	5.9	13.3	13.3	16.4	1	8	8	27	21	28	44	7	4	4
N. rudis	IRSNB18432	Wayalayeng	M	75.9	144.9	17.0	12.4	10.2	36.6	23.6	38.3	1	10	8	29	18	28	48	7	4	3
N. rudis	IRSNB18433	Maringma-tepui	M	73.6	127.0	17.0	11.3	12.1	34.0	22.8	39.9	2	7	8	28	16	27	51	8	4	3
N. rudis	IRSNB18434	Maringma-tepui	F	69.9	34.9	16.5	10.5	10.6	29.5	28.5	44.3	1	9	8	27	22	33	41	8	4	3
N. rudis	IRSNB18435	Maringma-tepui	M	80.5	147.0	19.1	12.1	13.1	36.8	30.7	45.8	2	10	8	30	20	35	55	9	5	3
N. rudis	IRSNB18436	Maringma-tepui	F	74.1	157.9	16.1	9.5	11.7	34.9	27.9	39.0	1	8	8	28	19	28	40	5	5	4
N. rudis	IRSNB18437	Maringma-tepui	M	53.4	92.3	12.4	7.5	8.9	24.1	20.0	30.1	2	8	8	29	21	29	51	8	4	3
N. rudis	IRSNB18438	Maringma-tepui	F	79.8	150.2	17.4	11.4	11.5	38.2	29.2	53.1	2	8	8	29	21	32	24	7	4	4
N. rudis UCS 1	CPI11021	Wokomung	M	73.7	92.8	17.6	11.0	13.6	35.2	24.9	38.6	1	6	8	29	15	26	48	6	3	4
N. rudis UCS 1	CPI11067	Wokomung	M	83.3	172.0	19.2	12.5	15.2	35.4	30.7	45.2	1	6	8	30	18	26	52	7	3	4
N. rudis UCS 1	CPI11068	Wokomung	F	61.4	127.0	14.4	9.1	10.9	28.7	21.9	34.6	1	6	8	28	19	32	39	8	4	4
N. rudis UCS 1	CPI11069	Wokomung	M	78.6	142.0	18.7	12.0	12.8	36.6	28.4	44.2	1	8	8	28	20	29	43	7	4	4
N. rudis UCS 1	IRSNB17344	Kaieteur	M	62.4	134.8	15.2	9.1	9.9	25.9	20.9	33.6	2	6	8	27	16	26	59	7	3	4
N. rudis UCS 1	IRSNB17056	Kaieteur	JUV	37.4	37.3	9.4	5.9	6.5	17.4	12.1	19.5	2	7	8	26	16	27	52	8	3	4
N. rudis UCS 1	IRSNB17057	Kaieteur	M	63.2	128.1	14.9	9.3	12.0	26.1	21.3	33.8	2	9	8	30	22	29	55	9	4	4
N. rudis UCS 1	IRSNB17346	Kaieteur	JUV	39.0	73.1	9.9	6.1	7.6	15.7	12.9	19.6	2	6	8	27	20	30	50	8	4	3
N. rudis UCS 1	IRSNB17347	Kaieteur	F	56.4	NA	14.5	8.7	10.0	25.0	22.4	34.1	2	11	8	27	20	28	41	7	4	4
N. rudis UCS 1	IRSNB18439	Iwokrama	F	52.9	103.9	12.1	7.3	7.8	24.4	18.1	28.4	2	10	8	28	20	29	58	8	3	4
N. rudis UCS 2	IRSNB18440	Iwokrama	M	63.3	26.1	15.6	10.0	9.6	29.6	20.0	34.1	2	9	8	28	14	29	47	7	4	4
N. rudis UCS 2	IRSNB18441	Iwokrama	F	47.3	NA	12.5	7.6	7.1	20.3	16.8	24.4	2	9	8	26	17	26	42	8	4	3
N. rudis UCS 2	IRSNB18442	Iwokrama	JUV	40.0	76.0	9.9	6.5	5.8	17.8	13.8	21.6	2	5	8	28	19	29	50	8	4	3
N. rudis UCS 2	IRSNB18443	Iwokrama	M	67.6	108.5	15.6	9.8	10.4	29.6	23.6	36.3	2	6	8	28	20	28	45	8	3	4
N. rudis UCS 2	IRSNB18444	Iwokrama	JUV	36.9	49.7	9.6	6.0	5.7	15.7	12.0	19.2	1	6	8	28	17	28	NA	7	3	3
N. rudis UCS 2	IRSNB18445	Iwokrama	JUV	44.5	NA	10.7	7.2	7.7	18.6	13.6	22.1	2	7	8	28	15	26	42	6	3	4
N. rudis UCS 2	IRSNB18446	Iwokrama	M	69.7	134.4	17.8	10.9	11.7	31.2	25.2	38.8	2	8	8	28	18	28	44	6	4	4
N. rudis UCS 2	IRSNB18447	Iwokrama	F	57.9	NA	13.1	8.5	9.6	27.5	18.1	28.6	2	7	8	26	17	27	42	6	3	4
N. rudis UCS 2	IRSNB18448	Iwokrama	M	70.6	NA	16.1	10.4	12.3	32.5	22.3	33.7	2	6	8	26	18	26	47	6	3	4
N. rudis UCS 2	IRSNB18449	Iwokrama	JUV	43.8	65.7	11.2	6.8	7.5	19.6	14.0	21.8	1	7	8	31	16	27	44	6	3	4
N. arekuna sp. nov.	IRSNB2688	Angasima-tepui	JUV	36.3	67.5	9.8	5.9	5.2	16.1	12.5	16.4	1	6	8	26	20	26	34	8	3	4
N. arekuna sp. nov.	IRSNB2689	Angasima-tepui	JUV	35.2	68.9	9.0	5.7	4.4	15.7	13.9	16.8	1	5	8	25	19	33	41	9	4	3

(*Continued*)

Table 2. (Continued).

Taxon	Museum voucher	Locality	Sex	SVL	TL	HL	HW	NL	AXG	FiL	HiL	Fn	Oc	VL	VT	SLF	SLT	FP	SL	IL	SO
N. arekuna sp. nov.	IRSNB2687	Angasima-tepui	F	74.5	97.5	17.2	9.8	9.7	35.6	26.2	37.8	1	4	8	27	21	29	36	8	4	4
N. arekuna sp. nov.	IRSNB2690	Angasima-tepui	M	63.0	130.7	14.0	9.4	10.2	30.5	20.5	31.6	1	4	8	26	18	27	51	8	4	3
N. arekuna sp. nov.	MZUSP106223	Pacaraima	M	63.1	NA	16.2	9.6	10.2	29.2	20.9	33.9	1	6	8	26	21	26	45	7	4	4
N. arekuna sp. nov.	MZUSP106224	Pacaraima	F	66.3	NA	18.8	9.7	10.5	33.8	21.9	35.0	1	7	8	26	18	25	43	7	4	4
N. arekuna sp. nov.	MZUSP106225	Pacaraima	JUV	48.4	96.7	13.2	7.4	7.2	23.2	17.0	25.1	1	5	8	27	19	27	41	7	5	4
N. arekuna sp. nov.	MZUSP106226	Pacaraima	M	70.2	NA	17.8	11.1	11.1	32.8	24.5	39.8	1	5	8	25	20	30	51	7	4	4
N. arekuna sp. nov.	MZUSP106227	Pacaraima	F	62.2	NA	15.4	8.8	11.1	30.1	20.0	32.7	1	6	8	25	19	29	42	6	4	4
N. arekuna UCS 1	IRSNB18450	Chivatón	M	80.6	144.3	17.9	12.1	11.1	37.0	25.9	36.6	1	4	8	27	16	27	40	7	3	4
N. arekuna UCS 1	IRSNB18451	Chivatón	JUV	39.7	77.7	10.0	6.3	5.9	17.8	12.3	18.8	1	9	8	29	18	26	46	7	4	3
N. arekuna UCS 1	IRSNB18452	Chivatón	M	74.7	107.5	17.9	11.3	10.6	33.9	25.1	38.5	1	8	8	27	19	29	47	8	4	3
N. arekuna UCS 1	IRSNB18150	Abakapá-tepui	M	70.0	128.4	17.7	10.7	9.1	32.1	23.7	35.8	1	7	8	26	19	25	44	8	4	3
N. arekuna UCS 1	IRSNB18453	Abakapá-tepui	JUV	39.1	36.0	10.0	6.1	5.4	17.1	14.4	19.1	1	4	8	23	20	27	47	8	4	3
N. arekuna UCS 1	IRSNB18454	Abakapá-tepui	JUV	44.2	43.8	11.0	6.9	6.6	18.8	15.3	22.1	1	7	8	26	17	26	46	8	4	4
N. arekuna UCS 2	IRSNB18109	El Danto	F	52.3	73.1	12.8	8.7	8.4	22.2	20.9	29.6	1	6	8	27	20	29	NA	8	4	3
N. arekuna UCS 2	IRSNB18110	La Escalera	F	69.4	130.3	15.0	9.4	10.2	31.1	23.8	35.3	1	8	8	27	21	29	44	8	4	4
N. arekuna UCS 2	IRSNB18111	La Escalera	F	70.2	126.7	15.4	10.0	9.5	32.4	24.8	36.4	1	4	8	28	19	29	41	8	4	3
N. arekuna UCS 2	MZUSP49193	La Escalera	F	70.8	105.2	15.8	9.6	11.6	33.1	22.6	33.9	1	6	8	26	20	28	49	7	4	NA
N. arekuna UCS 3	IRSNB18455	Auyán-tepui	F	81.0	163.6	18.4	11.9	11.2	37.2	28.7	46.3	1	6	8	28	20	30	48	7	4	4
N. arekuna UCS 3	IRSNB18456	Auyán-tepui	F	65.8	137.6	14.3	9.3	11.2	30.8	23.4	36.5	1	5	8	28	19	27	42	7	4	3

containing samples from Chivatón and the summit of Abakapá-tepui (Bolívar state, Venezuela; PP = 1) and one subclade containing samples from the La Escalera region and the summit of Auyán-tepui (Bolívar state, Venezuela; PP = 0.87). The clade east of the Gran Sabana (PP = 0.89, shown in red in Figure 2) is more structured, with four distinct subclades moderately to highly supported (PP 0.91–1.0, see Figure 2). Samples from Kaieteur National Park (KNP) are not recovered monophyletic, two samples (IRSNB17345 and ROM20514) are nested in a clade (PP = 1) 'basal' to the rest of the eastern clade, and one sample (IRSNB17344) is recovered sister to our sample from Mount Wokomung (ROM42644) in a clade (PP = 0.99) sister to a clade (PP = 1) containing samples from the Iwokrama Mountains in Guyana. That clade (KNP/Wokomung + Iwokrama; PP = 0.99) is sister to a clade containing samples from Maringma-tepui (ca. 15 km airline from the type locality of *N. rudis*) + Mount Ayanganna in west-central Guyana (PP = 0.91).

The species tree analysis (Figure 2) yielded a consensus tree with similar support and topology to the concatenated analysis, except for the position of *Neusticurus racenisi*, which is recovered 'basal' to the western and eastern clades of *N. rudis* with low support (PP = 0.55) instead of sister to the clade containing *N. bicarinatus* and *N. surinamensis* in the concatenated analysis (PP = 0.58). The DensiTree representation of the species tree (Figure 2) shows low uncertainty in the position of *N. rudis* from Kaieteur National Park, Guyana, when all specimens from Kaieteur are considered a single species.

Our analysis of C-mos alone did not resolve relationships among populations (not shown).

Genetic distances

Genetic distances of 2–3% in 16S (Table 3) and 10–12% in ND4 (Table 4) were observed between the clades east and west of the Gran Sabana. Results given by the fast-evolving ND4 gene are worth mentioning. Although the populations from Angasima-tepui (Venezuela) and Pacaraima (Brazil) seem geographically and topographically isolated (ca. 107 km airline, tepui-summit vs uplands) the genetic divergence in ND4 between these populations is zero. By contrast, in the same clade, the population from Abakapá-tepui, which is geographically closer to Angasima-tepui (ca. 25 km airline), differs from the Angasima-tepui population by 5% in the same gene fragment. A similar scenario occurs in the eastern clade, where genetic divergence in ND4 can be as high as 6% among subclades.

External morphology and morphometrics

Our results indicate a rather conserved – although to some extent quite variable within populations – external morphology with all measurement ratios and scale/femoral pore counts broadly overlapping among the examined populations (see Table 2). Nevertheless, we identified the following relevant diagnostic characters: the number of occipital scales in contact with the posterior edge of parietals and interparietal, the condition of dorsal tubercles (continuous rows vs discontinuous rows), and the condition of caudal tubercles (the last dorsal tubercle of each verticil distinctly or not overlapping the next verticil) (see Figure 3). The combination of these three phenotypic traits unambiguously differentiates the population from Angasima-tepui (Venezuela) and Pacaraima (Brazil) from the holotype
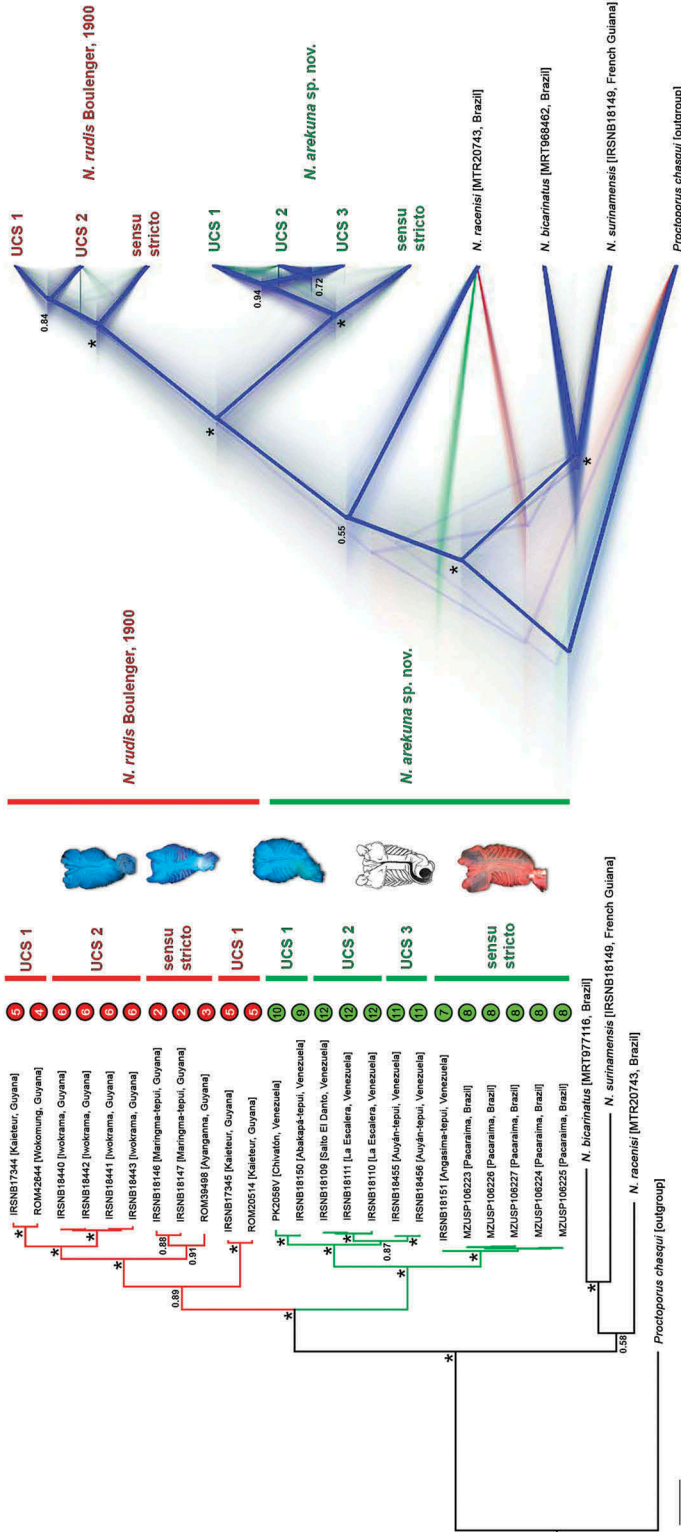
Figure 2. Bayesian tree of Pantepui *Neusticurus* obtained from the concatenated data set (left) and DensiTree representation of the species tree obtained from the *BEAST analysis (right). Numbers and colours correspond to those in Figure 1. Examined hemipenes are illustrated in front of the corresponding populations. Hemipenial drawing modified from Myers and Donnelly (2008). DensiTree representation: the most popular tree is blue; the next most popular tree is red; the third most popular tree is green. Asterisks indicate high posterior probabilities (values ≥ 99%). UCS = unconfirmed candidate species. Photos of hemipenes PMSN.

of *Neusticurus rudis* and populations from the vicinity of the type locality (Wayalayeng and Maringma-tepui).

Hemipenial morphology

Examination of hemipenial bodies yielded rather unexpected results. Although hemipenes were not available for every subclade, our results show that, when available, hemipenes sometimes substantially differ among most subclades, suggesting premating reproductive isolation (see below), even among genetically very close populations.

Taxonomic decision

Our molecular analyses revealed substantial phylogeographic structure within *Neusticurus rudis* in the eastern Pantepui region, suggesting the occurrence of more than one species under that name in the area. Our morphological data (external morphology, hemipenial morphology) corroborated this hypothesis with several subclades corresponding to phenotypically distinct populations. We were thus left with two main choices: naming all phenotypically distinct populations within each main clade as new, or naming only the two main clades. The first option seems premature as we currently do not have enough specimens to confidently decide whether the observed differences should be considered merely interpopulation variation or valid taxonomic divergences (for some populations only males or only females are available, and sometimes only a single specimen). Also, genetic divergence is often shallow within each of the two main clades (0–1% in our targeted fragment of the 16S, but up to 6% in our targeted fragment of the ND4; Tables 3–4). The second option is not entirely satisfactory either, first because the biological significance of phenotypical dissimilarities among populations cannot be ignored and second because these dissimilarities make it impossible to identify any unambiguous synapomorphy for each of the main clades. Therefore, in order to keep a stable taxonomy and avoid more confusion, we decided to redescribe *Neusticurus rudis* based only on the holotype and specimens from Wayalayeng and Maringma-tepui (Guyana) that are morphologically congruent with the holotype of *N. rudis* and geographically close from the type locality (ca. 15 km airline). We provisionally consider the other populations of the eastern clade as *N. rudis* sensu lato, but highlight morphological divergences among them and emphasise unconfirmed candidate species in our phylogenetic trees (Figure 2). Likewise, based on morphological and molecular evidence we describe the populations from Angasima-tepui, Venezuela, and Pacaraima, Brazil, as a new species; these populations are genetically divergent from *N. rudis* (2–3% on our targeted fragment of the 16S, 10–12% on our targeted fragment of the ND4; Tables 3–4), and differentiated by hemipenial morphology and subtle external morphological characters. At this stage, we consider other populations of the western clade to be *N. arekuna* sensu lato, but point out morphological divergences among them and emphasise unconfirmed candidate species in our phylogenetic trees (Figure 2) as we do for *N. rudis*.

Table 3. 16S uncorrected p-distance between taxa included in the phylogenetic analysis depicted in Figure 2.

	1	2	3	4	5	6	7	8	9	10	11	12	13	14	15	16	17	18	19	20	21	22	23	24	25	26
[1] *Neusticurus rudis* IRSNB18146	0																									
[2] *N. rudis* IRSNB18147	0.01	0																								
[3] *N. rudis* ROM39498	0.01	0.01	0																							
[4] *N. rudis* UCS 1 IRSNB17344	0.01	0.01	0.01	0																						
[5] *N. rudis* UCS 1 ROM42644	0.01	0.01	0.01	0	0																					
[6] *N. rudis* UCS 2 IRSNB18440	0	0	0.01	0	0.01	0																				
[7] *N. rudis* UCS 2 IRSNB18442	0	0	0.01	0	0.01	0	0																			
[8] *N. rudis* UCS 2 IRSNB18441	0	0	0.01	0	0.01	0	0	0																		
[9] *N. rudis* UCS 2 IRSNB18443	0	0	0.01	0	0.01	0	0	0	0																	
[10] *N. rudis* UCS 1 IRSNB17345	0.01	0.01	0.01	0.01	0.01	0.01	0.01	0.01	0.01	0																
[11] *N. rudis* UCS 1 ROM20514	0.01	0.01	0.01	0.01	0.01	0.01	0.01	0.01	0.01	0.03	0															
[12] *N. arekuna* IRSNB2688	0.02	0.02	0.02	0.02	0.02	0.02	0.02	0.02	0.02	0.03	0.03	0														
[13] *N. arekuna* MZUSP106223	0.02	0.02	0.02	0.02	0.02	0.02	0.02	0.02	0.02	0.03	0.03	0	0													
[14] *N. arekuna* MZUSP106226	0.02	0.02	0.02	0.02	0.02	0.02	0.02	0.02	0.02	0.03	0.03	0	0	0												
[15] *N. arekuna* MZUSP106227	0.02	0.02	0.02	0.02	0.02	0.02	0.02	0.02	0.02	0.03	0.03	0	0	0	0											
[16] *N. arekuna* MZUSP106224	0.02	0.02	0.02	0.02	0.02	0.02	0.02	0.02	0.02	0.03	0.03	0	0	0	0	0										
[17] *N. arekuna* MZUSP106225	0.02	0.02	0.02	0.02	0.02	0.02	0.02	0.02	0.02	0.03	0.03	0	0	0	0	0	0									
[18] *N. arekuna* UCS 1 PK2058V	0.02	0.02	0.02	0.02	0.02	0.02	0.02	0.02	0.02	0.03	0.03	0.01	0.01	0.01	0.01	0.01	0.01	0								
[19] *N. arekuna* UCS 1 IRSNB18150	0.02	0.02	0.02	0.02	0.02	0.02	0.02	0.02	0.02	0.02	0.03	0.01	0.01	0.01	0.01	0.01	0.01	0	0							
[20] *N. arekuna* UCS 2 IRSNB18109	0.02	0.02	0.02	0.02	0.02	0.02	0.02	0.02	0.02	0.02	0.03	0.01	0.01	0.01	0.01	0.01	0.01	0	0.01	0						
[21] *N. arekuna* UCS 2 IRSNB18111	0.02	0.02	0.02	0.02	0.02	0.02	0.02	0.02	0.02	0.02	0.03	0.01	0.01	0.01	0.01	0.01	0.01	0	0.01	0	0					
[22] *N. arekuna* UCS 2 IRSNB18110	0.02	0.02	0.02	0.02	0.02	0.02	0.02	0.02	0.02	0.02	0.03	0	0	0	0.01	0	0	0	0.01	0	0	0				
[23] *N. arekuna* UCS 3 IRSNB18455	0.02	0.02	0.02	0.02	0.02	0.02	0.02	0.02	0.02	0.02	0.03	0	0	0	0.01	0	0	0	0	0	0	0	0			
[24] *N. arekuna* UCS 3 IRSNB18456	0.02	0.02	0.02	0.02	0.02	0.02	0.02	0.02	0.02	0.02	0.03	0	0	0	0.01	0	0	0	0	0	0	0	0	0		
[25] *N. surinamensis* IRSNB18149	0.04	0.04	0.05	0.05	0.05	0.04	0.04	0.04	0.04	0.04	0.05	0.05	0.05	0.05	0.06	0.05	0.05	0.06	0.05	0.05	0.05	0.05	0.05	0.05	0	
[26] *N. bicarinatus* MRT977116	0.05	0.05	0.05	0.05	0.05	0.05	0.05	0.05	0.05	0.05	0.06	0.06	0.06	0.06	0.06	0.06	0.06	0.06	0.06	0.06	0.06	0.06	0.06	0.06	0.05	0
[27] *N. racenisi* MTR20743	0.05	0.05	0.04	0.05	0.05	0.05	0.05	0.05	0.05	0.05	0.05	0.06	0.06	0.06	0.06	0.06	0.06	0.07	0.06	0.06	0.06	0.06	0.06	0.06	0.06	0.06

Table 4. ND4 uncorrected p-distance between taxa included in the phylogenetic analysis depicted in Figure 2. Note that ND4 was not available for all samples.

	1	2	3	4	5	6	7	8	9	10	11	12	13	14	15	16	17	18	19	20
[1] *Neusticurus rudis* IRSNB18146																				
[2] *N. rudis* UCS 1 IRSNB17344	0.06																			
[3] *N. rudis* UCS 1 ROM42644	0.06	0.00																		
[4] *N. rudis* UCS 2 IRSNB18440	0.05	0.04	0.04																	
[5] *N. rudis* UCS 2 IRSNB18442	0.05	0.04	0.04	0.00																
[6] *N. rudis* UCS 2 IRSNB18441	0.05	0.04	0.04	0.00	0.00															
[7] *N. rudis* UCS 2 IRSNB18443	0.05	0.04	0.04	0.00	0.00	0.00														
[8] *N. arekuna* IRSNB2688	0.11	0.11	0.11	0.10	0.10	0.10	0.10													
[9] *N. arekuna* MZUSP106223	0.11	0.11	0.11	0.10	0.10	0.10	0.10	0.00												
[10] *N. arekuna* MZUSP106226	0.12	0.12	0.11	0.10	0.10	0.10	0.10	0.00	0.00											
[11] *N. arekuna* MZUSP106227	0.12	0.12	0.11	0.10	0.10	0.11	0.10	0.00	0.00	0.00										
[12] *N. arekuna* MZUSP106224	0.11	0.11	0.11	0.10	0.10	0.10	0.10	0.00	0.00	0.00	0.00									
[13] *N. arekuna* MZUSP106225	0.12	0.12	0.11	0.10	0.10	0.11	0.10	0.00	0.00	0.00	0.00	0.00								
[14] *N. arekuna* UCS 1 IRSNB18150	0.11	0.12	0.12	0.11	0.11	0.12	0.11	0.05	0.05	0.05	0.05	0.05	0.05							
[15] *N. arekuna* UCS 2 IRSNB18109	0.12	0.12	0.12	0.11	0.11	0.11	0.11	0.05	0.05	0.05	0.05	0.05	0.05	0.02						
[16] *N. arekuna* UCS 2 IRSNB18111	0.12	0.12	0.12	0.11	0.11	0.11	0.11	0.05	0.05	0.05	0.05	0.05	0.05	0.02	0.00					
[17] *N. arekuna* UCS 3 IRSNB18455	0.12	0.11	0.11	0.11	0.11	0.11	0.11	0.05	0.05	0.05	0.05	0.05	0.05	0.01	0.01	0.01				
[18] *N. surinamensis* IRSNB18149	0.17	0.18	0.18	0.17	0.17	0.17	0.17	0.16	0.17	0.17	0.17	0.17	0.17	0.17	0.17	0.17	0.17			
[19] *N. bicarinatus* MRT977116	0.20	0.21	0.20	0.21	0.20	0.21	0.21	0.19	0.19	0.19	0.19	0.19	0.19	0.19	0.19	0.19	0.19	0.20		
[20] *N. racenisi* MTR20743	0.17	0.17	0.16	0.15	0.15	0.16	0.15	0.15	0.15	0.15	0.15	0.15	0.15	0.16	0.16	0.16	0.16	0.18	0.19	

Note: For abbreviations see Table 2.
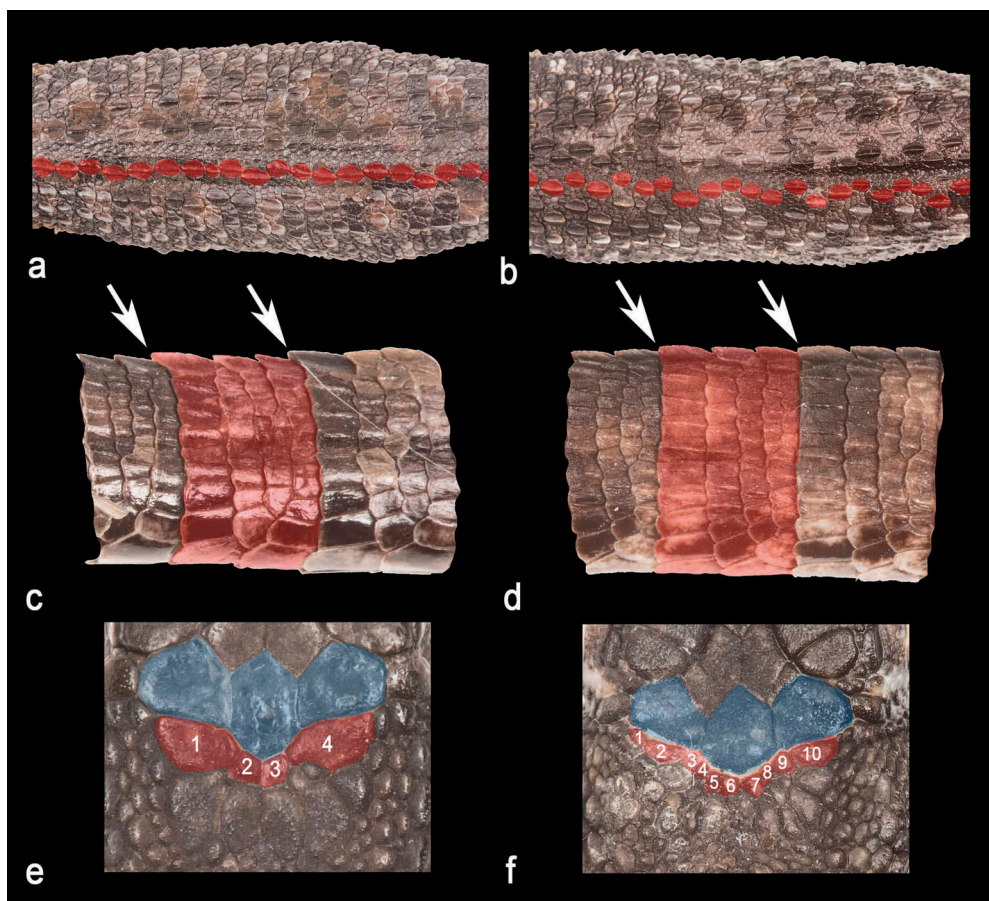
Figure 3. Relevant diagnostic characters to distinguish *Neusticurus arekuna* sp. nov. sensu stricto (left) from *N. rudis* sensu stricto (right). (a, b) Condition of dorsal tubercles. (c, d) Condition of caudal tubercles at the end of each verticil. (e, f) Number of occipital scales in contact with the posterior edge of parietals and interparietal. Photos PJRK, not to scale.

Systematic descriptions

<div align="center">

Family GYMNOPHTHALMIDAE Fitzinger, 1826
Genus ***Neusticurus*** Duméril and Bibron, 1839
Neusticurus rudis Boulenger, 1900
(Figures 4–6; Table 2)

</div>

Material examined

VENEZUELA. *Bolívar state*, Mount Roraima [± 1100 m elevation]: 1 adult ♂ (BM1946.8.31.64, holotype; high resolution digital photographs). GUYANA. *Cuyuni-Mazaruni district*, Wayalayeng [678 m elevation]: 1 adult ♂ (IRSNB18432) and 1 juvenile (IRSNB18431); slopes of Maringma-tepui [1060–1376 m elevation]: 4 adult ♂♂ (IRSNB18146, IRSNB18433, IRSNB18435, IRSNB18437) and 4 adult ♀♀ (IRSNB18147, IRSNB18434, IRSNB18436, IRSNB18438).

Referred material examined is listed in Table 2.

Note on the type locality of N. rudis

We follow the argument developed by Kok et al. (2018a) about specimens collected by F.V. McConnell and J.J. Quelch in 1898 at the foot of Mount Roraima, and consider the type locality of *N. rudis* to be on the southern slope of Mount Roraima in Bolívar state, Venezuela.

Diagnosis

Neusticurus rudis is characterised by the following combination of characters: (1) size moderate (maximum known SVL 80.5 mm); (2) tail 1.7–2.1 times SVL; (3) tympanum moderately recessed, auditory meatus short; (4) lower eyelid with semi-transparent disc of 5–8 palpebrals; (5) frontonasal single or paired; (6) occipital scales in contact with posterior edge of parietals and interparietal 7–11; (7) enlarged dorsal tubercles usually arranged in poorly defined, discontinuous longitudinal rows containing 41–45 scales; (8) flanks with enlarged trihedral scales, not forming distinct vertical rows, surrounded by smaller scales usually heterogeneous in size; (9) ventral scales in 25–30 transverse rows; (10) subdigital lamellae under 4th finger 16–22; (11) subdigital lamellae under 4th toe 27–35; (12) total number of femoral pores in males 40–55, 24–49 in females; (13) tail compressed with 4–5 transverse rows of lateral scales corresponding to two subcaudal scales and 2–3 dorsal tubercles (= verticils), the last dorsal tubercle of each verticil poorly overlapping the next verticil; (14) hemipenis non-capitate, lacking capitular groove on sides; (15) hemipenial lobes elongate with pointed tips, lacking lobular knobs.

Comparison with congeneric species

Neusticurus rudis is immediately distinguished from *N. bicarinatus, N. medemi* and *N. racenisi* in having the tympanum moderately recessed (deeply recessed in *N. bicarinatus, N. medemi* and *N. racenisi*), and by a larger number of femoral pores in females (24–49 in *N. rudis* vs 4–15 in *N. bicarinatus*, 9–10 in *N. medemi*, and 10–15 in *N. racenisi*). *Neusticurus rudis* is further distinguished from *N. medemi* and *N. racenisi*, and also from *N. tatei*, in having enlarged tubercles on the dorsum (absent in *N. tatei, N. medemi* and *N. racenisi*), and from *N. tatei* in having fewer femoral pores in males (40–55 in *N. rudis* vs 60–61 in *N. tatei*) and a larger number of femoral pores in females (24–49 in *N. rudis* vs eight in *N. tatei*). *Neusticurus rudis* is principally distinguished from *N. surinamensis* in having enlarged dorsal tubercles usually arranged in poorly defined, discontinuous longitudinal rows containing 41–45 scales (dorsal tubercles arranged in well-defined, straight and continuous longitudinal rows containing 30–41 scales in *N. surinamensis*), and by a larger number of femoral pores in females (24–49 in *N. rudis* vs 6–10 in *N. surinamensis*). *Neusticurus rudis* is further distinguished from *N. bicarinatus* and *N. surinamensis* by non-capitate and non-enlarged lobes on the hemipenis (hemipenis with lobes distinctly enlarged, capitate and detached from the hemipenial body in *N. bicarinatus* and *N. surinamensis*). *Neusticurus rudis* can be further distinguished from *N. medemi, N. racenisi* and *N. tatei* by having flounces of the hemipenial body divided by a nude area in the centre of the asulcate face (not interrupted in *N. medemi, N. racenisi* and *N. tatei*).

Redescription

A *Neusticurus* of moderate size (Figure 4), maximum SVL 80.5 mm in males, 79.8 mm in females. Tympanum moderately recessed, external auditory meatus short. Rostral well visible from above, wider than long, rounded anteriorly, in contact with first supralabials, nasal and frontonasal. Frontonasal pentagonal, single or paired, laterally in contact with nasal and loreal, posteriorly in contact with prefrontals; if single, frontonasal may be partly divided anteriorly; when paired, the two frontonasals are similar in shape. An azygous scale is found between the frontonasal(s) and the prefrontals in six of the 11 specimens examined (55%). Prefrontals irregularly pentagonal or hexagonal, in broad contact medially, anteriorly in contact with frontonasal(s), laterally in contact with loreal, first supraciliary and first supraocular, posteriorly in contact with frontal; prefrontals with an azygous scale between them in three of the 11 specimens examined and two azygous scales between them in one specimen. Frontal longer than wide, bell-shaped, irregularly hexagonal, wider anteriorly, partially divided in three of the 11 specimens examined, anteriorly divided into several smaller scales in one specimen, in contact with prefrontals, frontoparietals and three anteriormost supraoculars. A pair of irregularly pentagonal, rarely rhomboidal (one specimen), frontoparietals in broad contact medially, in contact with frontal, the two posteriormost supraoculars, parietals and interparietal; frontoparietals sometimes divided into multiple smaller scales; suture between frontoparietals indented by interparietal. Interparietal large, longer than wide, hexagonal to rhomboidal; short grooves in interparietal present in only two of the 11 specimens examined; interparietal projecting further posteriorly than parietals. Parietals variable in shape, irregularly pentagonal to rhomboidal, as wide as, or slightly wider than, the interparietal. Numerous occipitals highly variable in shape and size, 7–11 in contact with posterior edge of parietals and interparietal. Supraoculars four, the anteriormost smaller and often divided into two or more small scales or granules; occasionally one or two granules between 2nd supraocular and frontal; 1st supraocular contacting prefrontal, frontal and two anteriormost supraciliaries, rarely in point contact with loreal; 2nd supraocular in contact with 2nd and 3rd supraciliaries, and with frontal; 3rd supraocular in contact with frontal and frontoparietal, usually separated from supraciliaries by a row of small scales; 4th supraocular in contact with frontoparietal and parietal, rarely in contact with 5th and/or 6th supraciliaries. Supraciliaries 4–8, usually 5–6. Canthus rostralis well defined, nasal irregularly quadrangular or pentagonal, undivided, nostril near the centre, in contact with rostral (separated from rostral by two scales in one specimen), 1st supralabial (and 2nd supralabial in one specimen), loreal (or its lower segment when present), and frontonasal. Loreal irregularly quadrangular or pentagonal, usually divided in two scales by a horizontal suture (sometimes on one side only), the lower segment smaller; loreal – or its lower segment when present – in contact with 2nd and 3rd supralabials in one specimen, with 2nd supralabial in one specimen, with nasal, 1st supraciliary, frontonasal, prefrontal, frenocular and one or two preocular granules/scales. Frenocular pentagonal, usually longer than high (rarely higher than long), in contact with preocular granules/scales, loreal, 2nd and 3rd supralabials, followed by three – rarely two or four – usually subequal suboculars (second enlarged in a few specimens, first the smallest when four suboculars occur). Usually 5–6 postoculars, but up to eight in a few specimens (in these specimens several postoculars are highly reduced and granular), uppermost postocular the largest, in contact with temporals, parietal (although separated from parietal by one scale in one specimen), and separated from supraciliaries and supraoculars by a few

granular scales. Translucent palpebral disc with 5–8 palpebrals. Supralabials seven or eight, rarely five or nine; posteriormost 2–3 supralabials usually rounded with a blunt keel. Temporal region with juxtaposed scales, heterogeneous in size and shape, some keeled, especially in males (keels occur in a few females). Cephalic scales smooth, with small sensory pits along their edges, except on most anterior and lateral scales on which pits are usually more homogeneously distributed over the scales. Ear opening large, anterior border ellipsoid, posterior border straight, auditory meatus short.

Mental wider than long, rounded anteriorly, straight posteriorly. Postmental pentagonal, usually pointed posteriorly, wider than long, posteriorly in contact with a pair of genials, laterally in contact with 1st and 2nd infralabials (with 1st infralabial only in two of the 11 specimens examined). Two pairs of genials (chinshields), 1st pair in broad contact medially (except in three of the 11 specimens examined in which the 1st pair is separated by an elongate medial scale), laterally in contact with infralabials; 2nd pair smaller, medially separated by 3–4 small scales; both pairs in broad contact with infralabials; second pair of genials followed by a row of 2–4 enlarged scales. Infralabials 3–4. Pre-gulars smooth, round to ovoid, juxtaposed, slightly increasing in size laterally. A distinct (rarely indistinct) line of small scales, 2–4 scales wide, separate gulars from pre-gulars. Gulars smooth, smaller anteriorly, increasing in size posteriorly, smaller scales juxtaposed, larger scales imbricate. One row of paired enlarged gulars. Collar distinct, containing 6–8 enlarged scales, collar fold covered with smooth juxtaposed granules.

Neck covered with trihedral tubercles, in contact longitudinally, arranged in continuous rows separated by a series of small, irregularly disposed and juxtaposed scales. Lateral neck scales strongly protruded, trihedral, usually arranged in rows as on dorsal surface of neck. Dorsum covered with two different types of scales: (1) small, juxtaposed smooth or weakly keeled scales, and (2) large, prominently keeled ovoid tubercles. Dorsal tubercles usually disposed very irregularly, occasionally arranged in semi–longitudinal rows of 41–45 scales (from occipital scales to posterior margin of hind limb). If so, tubercles often misaligned. Tubercles smaller and more rounded dorsolaterally, becoming conical, although still keeled, on flanks where they are rarely arranged in poorly defined oblique (one specimen) or longitudinal (three specimens) rows. Ventrals smooth, slightly imbricate, rounded posteriorly in 25–30 transverse and eight longitudinal rows (including one row of 'lateral scales' on each side). Scales on preanal plate equal to, or smaller than, ventral scales, mostly pentagonal, diamond-shaped or convex posteriorly. Preanal scale pattern highly variable, in most specimens median scale largest, overlapping a smaller posterior scale. The latter is part of a transverse row of 5–7 (mostly five) scales delineating the posterior margin of the preanal plate. Median scale overlaps with two larger, quadrangular scales on the posterior margin of the plate. Multiple smaller, more or less rounded scales on the sides of the preanal plate, surrounding the scales mentioned above. Total number of femoral pores in males 40–55, 24–49 in females. Pores usually in a continuous row, separated from the preanal plate by 1–3 scales. Each femoral pore is surrounded by 4–5 small scales, which gives it a flower-like appearance.

Tail compressed, 1.7–2.1 times SVL, with a – usually discontinuous – double row of dorsal tubercles. Each tail segment (verticil) corresponds to two subcaudal scales and contains 4–5 transverse rows of keeled lateral scales and 2–3 keeled dorsal tubercles, the last dorsal tubercle of each verticil poorly overlapping the next verticil. Subcaudals smooth, imbricate, quadrangular and with convex posterior margin.

Figure 4. *Neusticurus rudis* sensu stricto in life. (a) Male from the slopes of Maringma-tepui (IRSNB18146). (b) Female from the slopes of Maringma-tepui (IRSNB18438). Photos PJRK.

Scales on dorsal surface of forelimbs weakly keeled, imbricate, with rhomboidal distal margin, arranged in longitudinal rows. Scales become smoother and smaller towards the ventral surface of the forelimbs. Scales on hand smooth, rhomboidal and strongly imbricate.

Hind limbs with keeled rhomboidal and imbricate scales anteriorly; proximal and posterior region covered with granular scales. Subdigital lamellae on hand and foot smooth and single; subdigital lamellae on foot slightly tuberculate at the base. Number of lamellae on 4th finger 16–22, on 4th toe 27–35. Palms and soles covered with small, granular scales.

The hemipenis of IRSNB18432 (Figure 5) is bilobed, with the hemipenial body ornamented with eight transverse flounces with no vestige of spines or any other calcified structure. Hemipenial body roughly conical, with the base thinner than the distalmost portion. Lobes not distinctly detached from hemipenial body, non-capitate and with pointed tips, which gives an overall Y-shape to the organ. The sulcus spermaticus is deep and central in position, originating at the base of the organ, and proceeding in a straight line towards the lobular basis, bifurcating just before the lobular crotch. A small and V-shaped fleshy fold divides the sulcus, and the resulting branches extend across the lobes, ending on the ventral face of each lobular tip, between two conspicuous knobs. Two narrow areas with no ornamentation are parallel to the sulcus spermaticus. A narrow nude area separates the eight hemipenial body transversal flounces in two lateral sets on the asulcate face. Each of the body flounces runs downwards from the sulcate face, changing its direction upwards and returning to the downward direction on the sides towards the asulcate face, making a W shape.

Sexual dimorphism present, females slimmer than males, usually smaller, head of males larger and broader, neck much narrower in relation to head (Figure 6). Maximum number of femoral pores higher in males, variation in femoral pores greater in females (24–49) than in males (40–55). Colour pattern similar in both sexes, males sometimes darker than females and/or with brighter colour on lower sides of head (Figures 4 and 6).

Colour in life (Figure 4)

Ground colour variable, brown, olive green, or grey; top of head grey or black. Scales on sides of head usually grey or greyish brown. Labials and lateroventral scales reddish brown, orange, beige or yellowish. Iris grey or reddish brown. Area encircling the eyes usually orange or yellow, especially below the eye and in the preocular and postocular region. Chinshields, pregulars and gulars mottled grey and white, often with a hint of orange or yellow. Sides of neck dark brown, with yellowish-ochre spots. Dorsal pattern usually uniformly dark brown, occasionally greyish brown with numerous irregular black spots on the middorsal line. Middorsal line covered with quadrangular to circular markings bordered with black. Flanks often with numerous white ocelli. Flanks becoming more reddish brown towards the ventral side of the body. Upper surface of limbs similar to the dorsal region, with multiple ill-defined spots on the sides. Ventral surface of body bluish white or beige, often with brown markings laterally. Underside of limbs white or beige, without flecks. Palms and soles brown or grey. Tail often light brown proximally, becoming heavily spotted distally. In juveniles, the middorsal part of the tail is often reddish brown.

Colour in preservative

Males and females uniform light or dark brown, dorsal part of head dark grey. Dorsal and dorsolateral region of back and tail often with numerous irregular dark grey flecks. Flanks lighter, greyish white scales often occurring ventrolaterally. Ventral part of head

white or beige, chinshields often mottled with brown or grey flecks. Ventral scales white or beige, ventrolaterals frequently with greyish spots. Underside of limbs white or beige. Tail white anteriorly, becoming brown or dark grey posteriorly.

Geographic variation within the N. rudis clade (Figures 7–8; Table 2)

There is some variation among the three localities under study in this clade (see also Discussion).

All specimens from Kaieteur National Park, Guyana (*Neusticurus rudis* UCS 1, 200–580 m elevation, Figure 7) have paired frontonasals and an azygous scale between frontonasals and prefrontals. Tubercles on the tail are smaller compared to those of specimens from other populations. Tubercles rarely imbricate at the base of the tail, mostly separated from the adjacent tubercle by 2–5 small, juxtaposed scales. Tubercles increase in number distally, frequently coming in contact with each other.

In specimens from the Iwokrama Mountains, Guyana (*N. rudis* UCS 2, 70–200 m elevation, Figure 7) the sexual dimorphism is much reduced (Figure 8, compared to Figure 6). Heads of males are distinctly narrower than those of males from Mount Roraima, Maringma-tepui and Kaieteur National Park (head width only slightly wider than neck vs distinctly wider in specimens from Mount Roraima, Maringma-tepui and Kaieteur National Park). Labials and region above supralabials are bluish white, with
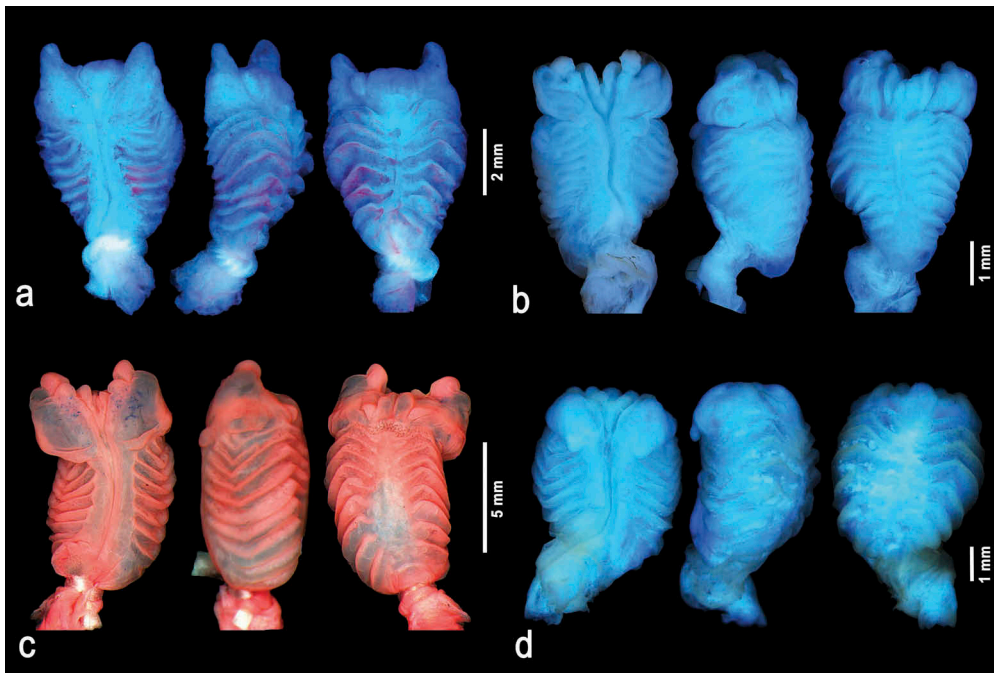
Figure 5. Variation of hemipenial bodies. (a) *Neusticurus rudis* sensu stricto from Maringma-tepui, Guyana (IRSNB18432). (b) *N. rudis* UCS 2 from Iwokrama, Guyana (IRSNB18446). (c) *N. arekuna* sp. nov. from Pacaraima, Brazil (MZUSP106223). (d) *N. arekuna* UCS 1 from Abakapá-tepui, Venezuela (IRSNB18150). Photos PMSN.
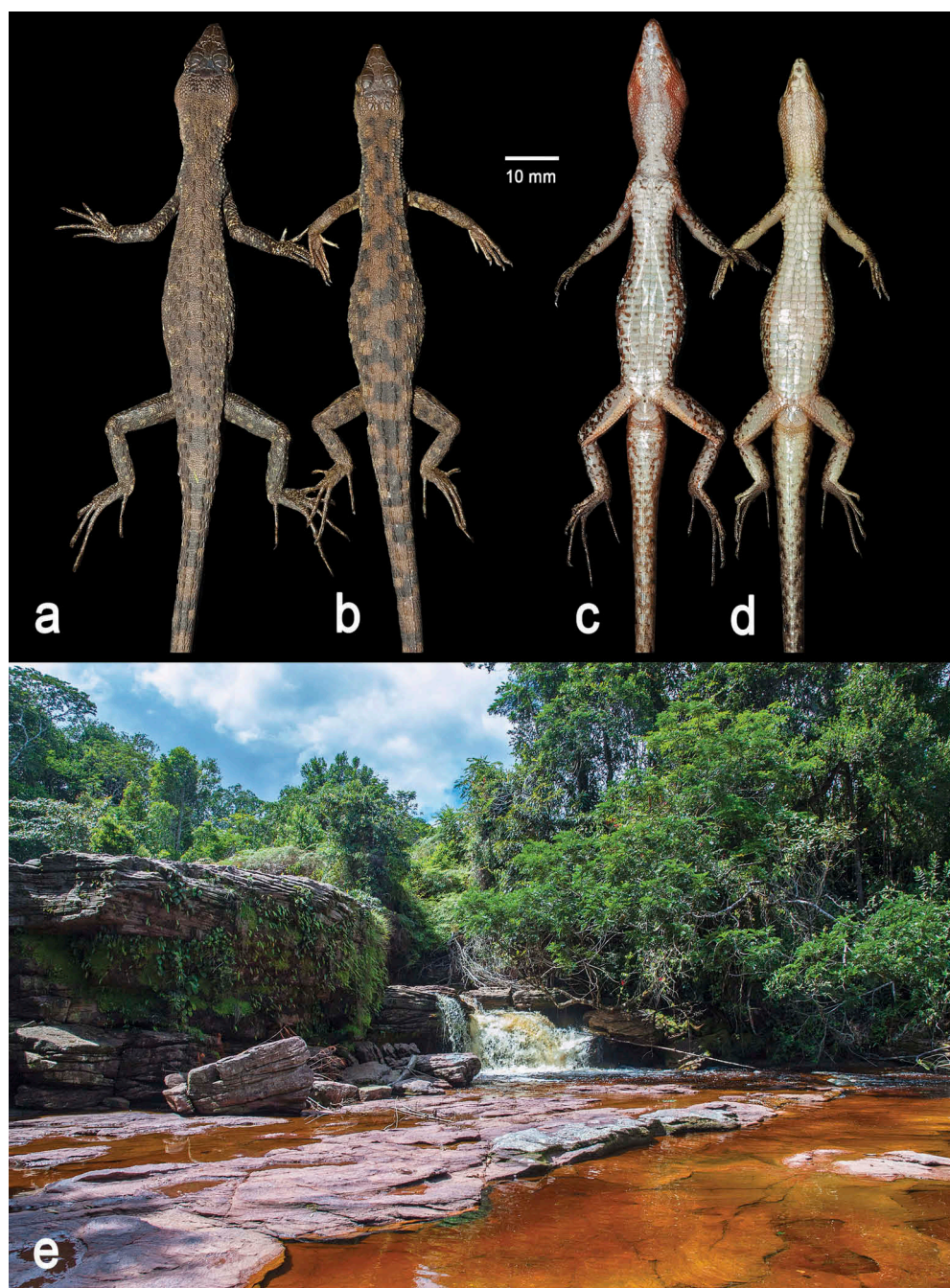
Figure 6. Sexual dimorphism and habitat of *Neusticurus rudis* sensu stricto. (a) Dorsal face of a male immediately after euthanasia (IRSNB18435). (b) Dorsal view of a female immediately after euthanasia (IRSNB18436). (c) Ventral view of a male immediately after euthanasia (IRSNB18435). (d) Ventral view of a female immediately after euthanasia (IRSNB18436). (e) Habitat along the Ataro river, Guyana (November 2007). Photos PJRK.

black or brown markings, extending onto the ventral side of the head. Sides of neck are beige or yellowish-ochre, with irregular pattern of dark brown markings or several rather large white spots. Ventral scales are creamy white to beige, nearly immaculate, occasionally with a few small flecks on the two lateralmost rows of scales. Occipital scales are fewer in specimens from the Iwokrama Mountains than in specimens from the other two localities.

Although hemipenes from the Kaieteur population are not available, there is substantial variation between the hemipenial organ of *N. rudis* sensu stricto and the organ of the Iwokrama population, mainly regarding the lobular shape and capitation. The hemipenis of the specimens from Iwokrama has distinctly capitate lobes, with the tips detached from the hemipenial body and ornamented with rounded knobs, whereas the hemipenis of *N. rudis* sensu stricto is non-capitate with no tip detached from the hemipenial body and no apical ornamentation (Figure 5).

Distribution and natural history

Neusticurus rudis sensu stricto as redefined here is currently restricted to east of the Venezuelan Gran Sabana, from the slopes of Mount Roraima in Venezuela through Wayalayeng and the slopes of Maringma-tepui to Mount Ayanganna in Guyana, between 678–1500 m elevation, a region drained by tributaries of the Essequibo and Mazaruni rivers (Figure 1). Other populations provisionally referred to that species (see above and Discussion) are currently found exclusively east of the Venezuelan Gran Sabana, from Mount Wokomung in the Pakaraima Mountains of Guyana to the Iwokrama Forest Reserve in Guyana between 159 and 1234 m elevation.

All specimens were found closely associated with streams in primary forest. The eight specimens collected on the slopes of Maringma-tepui were caught moving along the edges of cascading streams during the day, or sleeping on rocks along streams at night. Two specimens collected close to Wayalayeng were collected during the day on rocks in the Ataro River, at the top of Ataro Fall (Figure 6). Disturbed specimens quickly dove into the water.

Neusticurus arekuna sp. nov.
Neusticurus rudis Marques-Souza et al. (in press)
(Figures 5, 9–11; Table 2)

Holotype

IRSNB2687, an adult female collected on 11 May 2011 at 9:20 am by PJRK on the summit of Angasima-tepui (Bolívar state, Venezuela, 5°02.5833N, 62°04.8667W, ca. 2200 m elevation).

Paratypes (n = 8)

VENEZUELA. *Bolívar state*, summit of Angasima-tepui, (5°02.5833N, 62°04.8667W, ca. 2200 m elevation), one adult male (IRSNB2690) collected on 14 May 2011 by Brad Wilson and two juveniles (IRSNB2688 [formerly IRSNB18151], IRSNB2689) collected on 12 May and 13 May 2011, respectively, by PJRK. BRAZIL. *Roraima state*, Pacaraima (4°
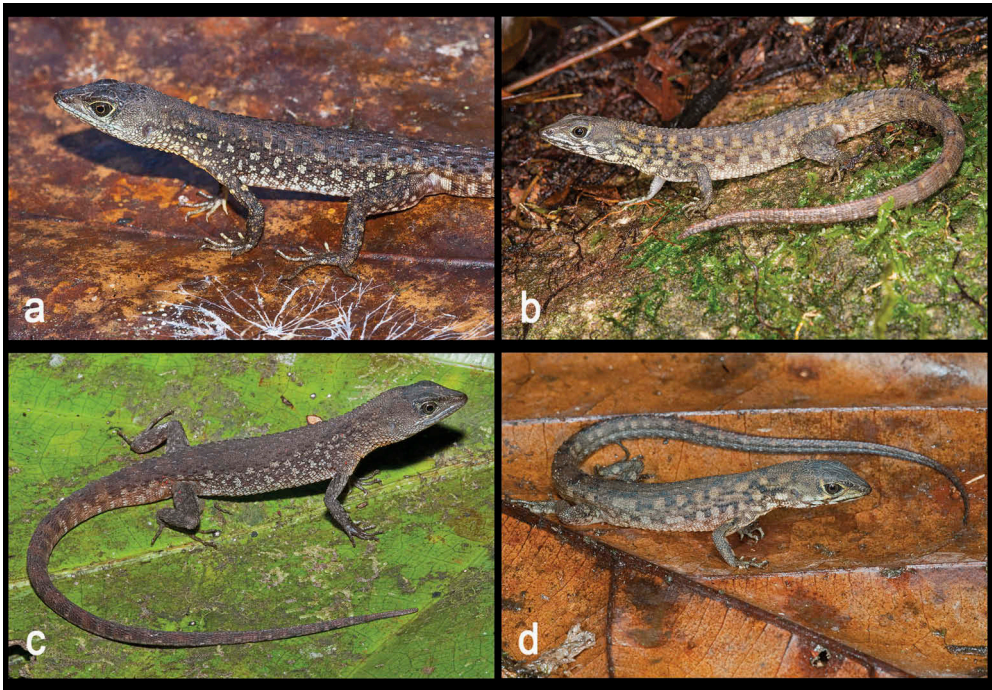
Figure 7. Variation in the *Neusticurus rudis* clade. (a) Male *N. rudis* UCS 1 from Kaieteur National Park, Guyana (IRSNB17344). (b) Male *N. rudis* UCS 2 from Iwokrama, Guyana (IRSNB18443). (c) Male *N. rudis* UCS 1 from Kaieteur National Park, Guyana (IRSNB17345). (d) Female *N. rudis* UCS 2 from Iwokrama, Guyana (IRSNB18441). Photos PJRK.

27.6333N, 61°08.7W, 900 m elevation), two adult males (MZUSP106223, MZUSP106226), two adult females (MZUSP106224, MZUSP106227), and one juvenile (MZUSP106225) collected in May 2011 by MTR, SMS, AF, MTJ, Augustín Camacho and Renato Recoder.

Referred material examined is listed in Table 2.

Etymology

The specific epithet is a noun in apposition honouring the Arekuna tribe (also known as the Pemon tribe) that lives in the region of Pantepui where the new species was collected.

Diagnosis

Neusticurus arekuna sp. nov. is characterised by the following combination of characters: (1) size moderate (maximum known SVL 74.5 mm in the holotype, IRSNB2687); (2) tail 1.7–2.1 times SVL; (3) tympanum moderately recessed, auditory meatus short; (4) lower eyelid with semi-transparent disc of 5–6 palpebrals; (5) frontonasal single; (6) occipital scales in contact with posterior edge of parietals and interparietal 4–7; (7) enlarged dorsal tubercles arranged in continuous, although sometimes poorly defined, longitudinal rows containing 40–44 scales;
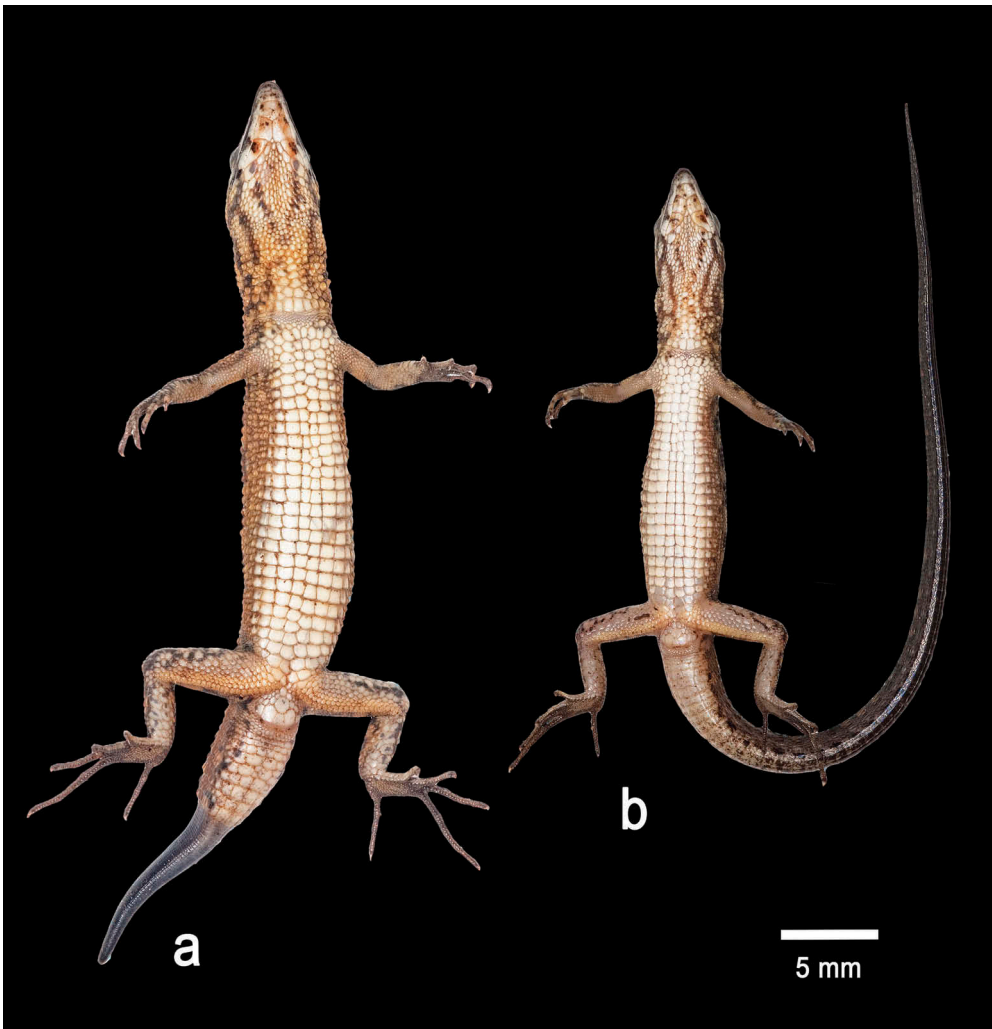
Figure 8. *Neusticurus rudis* UCS 2 from Iwokrama, Guyana. (a) ventral view of a male immediately after euthanasia (IRSN18440). (b) ventral view of a female immediately after euthanasia (IRSNB18441). Photos PJRK.

(8) flanks with large trihedral scales surrounded by smaller scales, heterogeneous in size; (9) ventral scales in 25–27 transverse rows; (10) subdigital lamellae under 4th finger 18–21; (11) subdigital lamellae under 4th toe 25–33; (12) total number of femoral pores 45–51 in males, 36–43 in females; (13) tail compressed with 4–5 transverse rows of lateral scales corresponding to two subcaudal scales and 2–3 dorsal tubercles (= verticils), the last dorsal tubercle of each verticil distinctly overlapping the next verticil; (14) hemipenis with lobes enlarged, distinctly capitate and detached from the hemipenial body; (15) hemipenis with all lateral flounces separated on the central asulcate face by an enlarged nude stripe that occupies ca. one third of the total asulcate face of the hemipenial body.
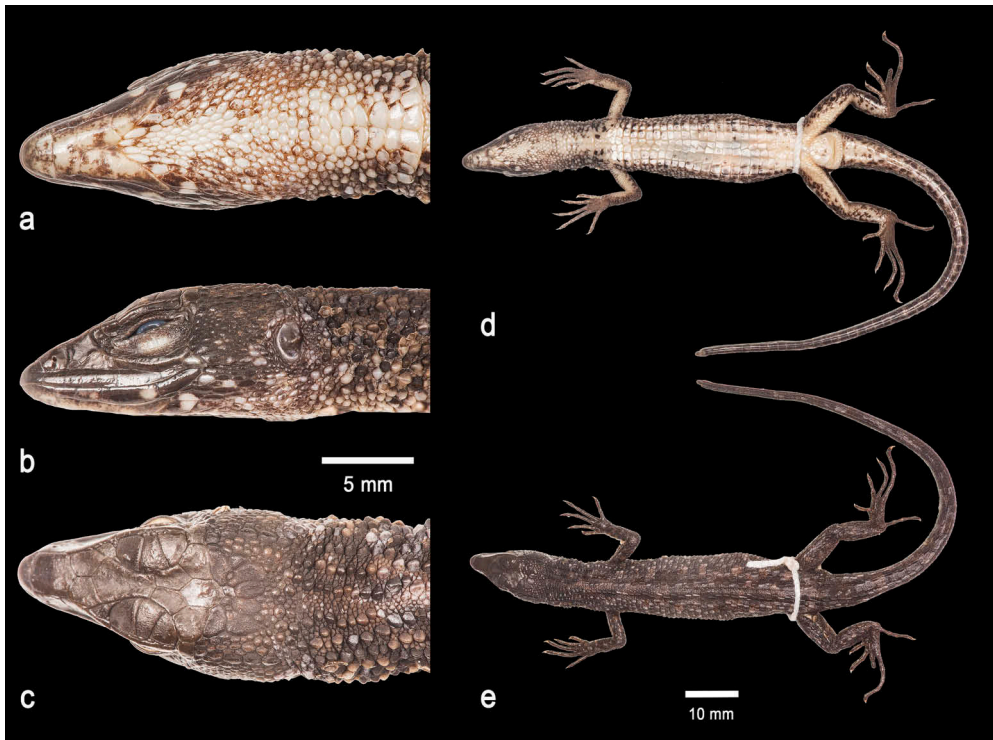
Figure 9. Holotype of *Neusticurus arekuna* sp. nov. (IRSNB2687) in preservative (a) Ventral view of head. (b) Lateral view of head. (c) Dorsal view of head. (d) Ventral view of body. (e) Dorsal view of body. Photos PJRK.

Comparison with congeneric species

Neusticurus arekuna sp. nov. is immediately distinguished from *N. bicarinatus, N. medemi* and *N. racenisi* in having the tympanum moderately recessed (deeply recessed in *N. bicarinatus, N. medemi* and *N. racenisi*), and by a larger number of femoral pores in females (36–43 in *N. arekuna* vs 4–15 in *N. bicarinatus*, 9–10 in *N. medemi* and 10–15 in *N. racenisi*). *Neusticurus arekuna* sp. nov. is readily distinguished from *N. medemi, N. tatei* and *N. racenisi* in having enlarged tubercles on dorsum (absent in *N. medemi, N. tatei* and *N. racenisi*). Further compared with *N. tatei, N. arekuna* sp. nov. has fewer femoral pores in males (45–51 in *N. arekuna* vs 60–61 in *N. tatei*), and a larger number of femoral pores in females (36–43 in *N. arekuna* vs eight in *N. tatei*). *Neusticurus arekuna* sp. nov. is immediately distinguished from *N. surinamensis* by having a larger number of femoral pores in females (36–43 in *N. arekuna* vs 6–10 in *N. surinamensis*) and by having a single frontonasal (divided in *N. surinamensis*). *Neusticurus arekuna* sp. nov. can be further distinguished from *N. medemi, N. racenisi* and *N. tatei* by having hemipenial lobes enlarged, capitate and detached from the hemipenial body, and in having the flounces of the hemipenial body divided by a nude area at the centre of the asulcate face (hemipenial lobes not enlarged, non-capitate, continuous with the hemipenial body, and flounces not interrupted in *N. medemi, N. racenisi* and *N. tatei*). *Neusticurus arekuna* sp. nov. is most similar to *N. rudis* from which it can be distinguished by the following
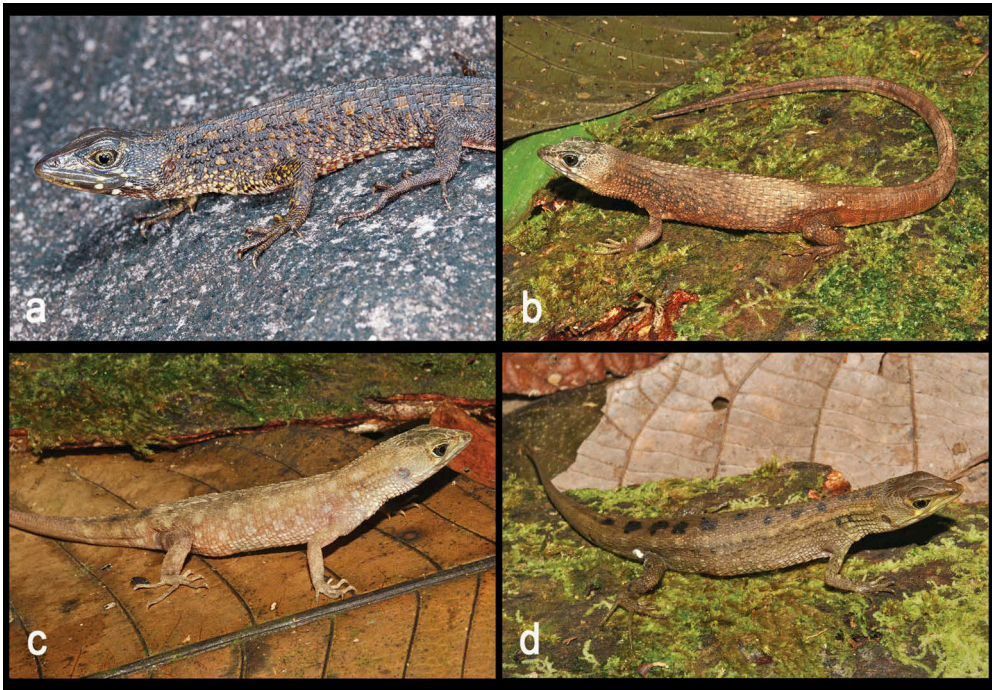
Figure 10. Variation among paratypes of *Neusticurus arekuna* sp. nov. (a) Female holotype in life (IRSNB2687). (b) Male paratype from Pacaraima, Brazil, in life (MZUSP106223). (c) Female paratype from Pacaraima, Brazil, in life (MZUSP106224). (d) Female paratype from Pacaraima, Brazil, in life (MZUSP106227). Photos PJRK (a), SMS (b–d).

combination of characters: enlarged dorsal tubercles arranged in well-defined, continuous longitudinal rows (usually arranged in poorly defined, discontinuous longitudinal rows in *N. rudis*) and last dorsal tubercle of each verticil distinctly overlapping the next verticil (poorly overlapping in *N. rudis*). *Neusticurus arekuna* sp. nov. is further distinguished from *N. bicarinatus* and *N. rudis* sensu stricto by having the hemipenial lobular tips ornamented with round knobs (hemipenial lobular tips lacking knobs or other visible ornamentation in *N. bicarinatus* and *N. rudis* sensu stricto).

Description of holotype
A female 74.5 mm SVL (Figures 9–10). Tympanum moderately recessed, external auditory meatus short. Rostral well visible from above, wider than long, rounded anteriorly, in contact with anterior supralabials, nasal and frontonasal. Frontonasal single, laterally in contact with nasal and loreal, posteriorly in contact with prefrontals. Prefrontals irregularly pentagonal, in broad contact medially, anteriorly in contact with frontonasal, laterally in contact with loreal, first supraciliary and first supraocular, posteriorly in contact with frontal. Frontal longer than wide, bell-shaped, hexagonal, wider anteriorly, in contact with prefrontals, first three supraoculars and frontoparietals. A pair of pentagonal frontoparietals in broad contact medially, in contact with frontal, the last two supraoculars, parietals and interparietal; suture between frontoparietals indented by interparietal. Interparietal large, longer than wide, roughly hexagonal; interparietal

Figure 11. Habitat of *Neusticurus arekuna* sp. nov. (a) Type locality on the summit of Angasima-tepui, Venezuela (looking east, May 2011). (b) Stream on the southern slope of the Serra Pacaraima, Roraima state, Brazil (May 2011). Photos PJRK (a) and SMS (b).

projecting farther posteriorly than the parietals. Parietals irregularly pentagonal, wider than interparietal. Occipitals variable in shape and size, four in contact with posterior edge of parietals and interparietal. Supraoculars four, the anteriormost smallest with two

small granules at the posterior angles; 1st supraocular contacting prefrontal, frontal and two first supraciliaries; 2nd supraocular in contact with 2nd and 3rd supraciliaries, and with frontal; 3rd supraocular in contact with frontal and frontoparietal, separated from supraciliaries by a row of small scales; 4th supraocular in contact with frontoparietal and parietal, in contact with 5th supraciliary on the left side and 6th supraciliary on the right side. Supraciliaries five on the left side, six on the right side. Canthus rostralis well-defined, nasal irregularly quadrangular, undivided, nostril near the centre, in contact with rostral, 1st supralabial, loreal (upper and lower segments), and frontonasal. Loreal irregularly pentagonal, divided in two by a horizontal suture, the lower segment smaller; lower segment of loreal in contact with 1st and 2nd supralabials and with nasal; upper segment of loreal in contact with 1st supraciliary, frontonasal, prefrontal, frenocular, and one preocular granules/scales. Frenocular pentagonal, longer than high, in contact with preocular granules/scales, both segments of loreal, 2nd and 3rd supralabials, followed by two suboculars, the 1st half the length of the second. Four postoculars on the right side, five on the left side, uppermost postocular the largest, in contact with temporals, parietal, and separated from supraciliaries and supraoculars by three granular scales on each side. Translucent palpebral disc with five palpebrals. Six supralabials on the right side, eight on the left side; supralabial behind eye the longest. Temporal region with juxtaposed scales, heterogeneous in size and shape, a few weakly keeled. Cephalic scales smooth, with small sensory pits along their edges, except on rostral, frontonasal, first supraocular and upper segment of the loreal on which pits are more homogeneously distributed over the scales. Ear opening large, anterior border ellipsoid, posterior border straight, auditory meatus short.

Mental wider than long, rounded anteriorly, straight posteriorly. Postmental pentagonal, pointed posteriorly, wider than long, posteriorly in contact with a pair of genials, laterally in contact with 1st and 2nd infralabials. Two pairs of genials (chinshields), 1st pair medially in broad contact, separated by a small medial scale posteriorly, laterally in contact with infralabials; 2nd pair narrower but longer, medially separated by four small scales; both pairs in broad contact with infralabials; second pair of genials followed by a row of three enlarged scales. Infralabials four. Pre-gulars smooth, round to ovoid, juxtaposed, slightly increasing in size laterally. No visible line of scales separates gulars from pre-gulars. Gulars smooth, slightly smaller anteriorly, increasing in size posteriorly, smaller scales juxtaposed, larger scales sometimes slightly imbricate. One row of paired enlarged gulars. Collar distinct, containing eight enlarged scales, collar fold covered with smooth juxtaposed granules.

Dorsum of neck covered with trihedral tubercles, in contact longitudinally, arranged in continuous rows separated by series of small, irregularly disposed and juxtaposed scales. Lateral neck scales strongly protruded, trihedral, arranged in longitudinal rows as on dorsal part of neck. Dorsum with two different types of scales: (1) small, juxtaposed smooth or slightly keeled scales, and (2) large, prominently keeled ovoid tubercles. Dorsal tubercles disposed rather regularly, arranged in longitudinal rows of 41 scales (from occipital scales to posterior margin of hind limb). Most tubercles aligned. Tubercles smaller and more rounded dorsolaterally, becoming conical, although still keeled, on flanks where they are arranged in poorly defined oblique rows anteriorly. Ventrals smooth, slightly imbricate, rounded posteriorly in 27 transverse and eight longitudinal rows (including one row of 'lateral scales' on each side). Scales on preanal

plate equal in size to, or smaller than, ventral scales, mostly pentagonal or irregularly quadrangular. Median scale largest, slightly overlapping a smaller posterior scale. The latter is part of a transverse row of seven scales delineating the posterior margin of the preanal plate. Two slightly smaller (about two thirds of the median scale), irregularly hexagonal scales on each side of the median scale. Two much smaller (about one fourth of the median scale), irregularly quadrangular scales anterior to median scale. Four small rounded or ovoid scales border the lateral margins of the preanal plate, the two anteriormost in contact with femoral pores. Total number of femoral pores 36, in a continuous row separated medially from the preanal plate by two scales. Most femoral pores surrounded by 4–6 small scales, giving it a flower-like appearance.

Tail compressed, incomplete, tip regenerating, with a continuous double row of tubercles. Each tail segment (verticil) corresponds to two subcaudal scales and contains 4–5 transverse rows of keeled lateral scales and 2–3 keeled dorsal tubercles, the last dorsal tubercle of each verticil distinctly overlapping the next verticil. Subcaudals smooth, imbricate, quadrangular and with convex posterior margin.

Scales on dorsal surface of forelimbs smooth or slightly keeled, imbricate, with rhomboidal distal margin, arranged in longitudinal rows. Scales become smoother and smaller towards the ventral surface of the forelimbs. Scales on hand smooth, rhomboidal and strongly imbricate. Hind limbs with keeled rhomboidal and imbricate scales anteriorly; proximal and posterior region covered with granular scales. Subdigital lamellae on hand and foot smooth and single; subdigital lamellae on foot slightly tuberculate at the base. Number of lamellae on 4th finger 21, on 4th toe 29. Palms and soles covered with small, granular scales.

Colour of holotype in life (Figure 10)

Head greenish brown dorsally and laterally, one vivid yellow spot on posterior of lower lip, under the eye; similar spots occur on the lower temporals and post-genial scales. Eye surrounded by a yellowish-brown ring; iris greenish. Dorsal ground colour of body and tail dark olive brown; a series of dorsolateral yellowish-ochre squarish spots extends from neck to ca. eighth verticil on tail. Light irregular yellowish-ochre spots on flanks corresponding to one or more tubercles, which in combination with the dorsolateral spots make an inconspicuous checked pattern. Limbs dark olive brown with scattered yellowish-ochre spots, posterior surface of thighs uniform dark brown. Ventral surface of head and throat creamy white with numerous dark brown markings, more extensive on genials and laterally. Venter whitish anteriorly and medially, with an orange tint posteriorly; irregular dark brown flecks on lateral ventral scales. Ventral surface of forelimbs greyish white, of hind limbs orangish-grey. Ventral surface of tail cream with numerous dark brown flecks increasing in number posteriorly where the tail becomes completely dark brown. Palms and soles dark brown.

Colour of holotype in preservative (Figure 9)

Similar to colour in life, but less vividly marked. Vivid yellow spots on upper and lower lip, on lower temporals and on post-genial scales became white. Dorsal surfaces mostly dark greyish-brown, yellowish-ochre markings became light brown. Ground colour of ventral surfaces more uniform, creamy white with dark brown markings as described above.

Hemipenis (Figure 5)

The hemipenis of the paratype MZUSP106223 (Pacaraima, Brazil) is bilobed, with the hemipenial body ornamented with 10 transversal flounces with no vestige of spines or any other calcified structure. Hemipenial body roughly cylindrical. Lobes distinctly detached from hemipenial body, capitate and with a pair of rounded knobs ornamenting the tip of each lobe. The lobular surface is nude, with no flounce or other ornamentation. The sulcus spermaticus is deep and central in position, originating at the base of the organ, and proceeding in a straight line towards the lobular basis, bifurcating just before the lobular crotch. A small V-shaped fleshy fold with conspicuous projections at the tip of the lobular crotch divides the sulcus, and the resulting branches extend across the lobes, ending between the knobs at lobular tips. Two narrow areas with no ornamentation are parallel to the sulcus spermaticus. A wide nude area separates the 10 hemipenial body transversal flounces into two lateral sets on the asulcate face. Each of the body flounces runs downwards from the sulcate face, changing its direction upwards and returning to the downward direction on the sides towards the asulcate face, making a Wshape. The preparation of a hemipenis of the paratype IRSNB2690 (Angasima-tepui, Venezuela) is suboptimal (inflation slightly incomplete), but hemipenial morphology is similar to MZUSP106223.

Variation in the type series (Figure 10)

Most variation in the type series is covered in the diagnosis; see also Table 2. All paratypes except two paratopotypes (IRSNB2688 and IRSNB2690) have an undivided loreal as in the holotype, making the undivided loreal the most common pattern in the species (found in 78% of the specimens examined). Compared to the holotype, other minor differences are found in the scalation: the interparietal may rarely be transversally divided; the two occipitals posterior to the interparietal are often dorsally elongated, crossing the whole occipital area. Occipital scales in contact with the posterior edge of parietals 4–7 (four in holotype). There is significant variation in colour pattern: ground dorsal colour varies from dark greenish/olive brown to chestnut brown and dorsal pattern varies from conspicuous to almost absent (Figure 10). Some of this variation could apparently be attributed to ontogeny or sexual dimorphism, although our sample is too small to support these conclusions. Juveniles are rather variable, one juvenile paratopotype (IRSNB2689) has a broad chestnut brown dorsal band and an inconspicuous series of dorsolateral ochre squarish spots as in the holotype. Additional discreet squarish spots on flanks make an inconspicuous checked pattern as in the holotype. The other juvenile paratopotype (IRSNB2688) lacks a dorsal band but also has an inconspicuous series of dorsolateral ochre squarish spots; no checked pattern occurs in that specimen. Among paratypes from Pacaraima, the checked pattern on flanks is visible in the juvenile (MZUSP106225) and in females (MZUSP106224, MZUSP106227), although less conspicuous in the latter. The checked pattern is absent in males from Pacaraima and inconspicuous in the male from Angasima-tepui.

Distribution and natural history

Neusticurus arekuna sp. nov. sensu stricto is currently only known from two localities west of the Venezuelan Gran Sabana: the summit of Angasima-tepui in Bolívar state, Venezuela (2162 m elevation), and a stream on the southern slope of the Serra Pacaraima in Roraima state, Brazil (900 m elevation, Figure 1). The unnamed stream flows into the Rio Surumu in

the Rio Branco Basin. The new species is expected to occur between these two localities. Other populations provisionally referred to that species (see above and Discussion) are currently found exclusively west of the Venezuelan Gran Sabana, from the La Escalera region to Chivatón, the summit of Abakapá-tepui, and the slopes and summit of Auyán-tepui, Venezuela, between 1100 and 2203 m elevation.

Neusticurus arekuna sp. nov. seems ecologically highly plastic as it was found in very different habitats and along a broad elevational range (Figure 11). Macrohabitat at the type locality (summit of Angasima-tepui) is characterised by tepui-summit scrub and meadows on peat and rock (McDiarmid and Donnelly 2005). All specimens at the type locality were collected by day; the holotype was swimming across a small puddle on rocks, IRSNB2688 was found under a rock, IRSNB2689 was found 170 cm above the ground on a rock wall and IRSNB2690 was collected walking among pitcher plants (*Heliamphora* sp). Other paratypes (from Pacaraima, Brazil) were found in a more typical habitat for *Neusticurus*, a cascading stream in primary forest, with large granitic boulders.

Geographic variation within the N. arekuna *clade (Figure 12; Table 2)*

Dorsal tubercles in adult specimens from Chivatón (*Neusticurus arekuna* UCS 1; two females) and the summit of Abakapá-tepui (*Neusticurus arekuna* UCS 1; one male) are generally larger (especially on the tail) and more strongly keeled than in specimens from other populations in the clade. Conversely, four adult female specimens from the La Escalera region (*Neusticurus arekuna* UCS 2) have distinctly smaller and less keeled dorsal tubercles than other populations in the clade; these tubercles are distributed in a similar way to those in the *rudis* clade (arranged in poorly defined, discontinuous longitudinal rows, see Figure 12) making confusion with *N. rudis* easy. Two adult female specimens from Auyán-tepui (*Neusticurus arekuna* UCS 3) are morphologically very similar to *Neusticurus arekuna* sp. nov. sensu stricto, and the two populations apparently have a similar hemipenial organ (as described in Myers and Donnelly 2008), while the hemipenis from the population of Abakapá-tepui shows significant differences compared to the hemipenis of *Neusticurus arekuna* sp. nov. sensu stricto, regarding the hemipenial body and lobular shapes. The hemipenis of the specimen from Abakapá-tepui (IRSNB18150) has distinctly reduced lobes, not detached from the hemipenial body or capitate; the lobular tips lack any visible ornamentation, but have a pair of knobs directed basally at the basis of their sulcate face. On the other hand, the hemipenis of the specimen of *Neusticurus arekuna* sp. nov. sensu stricto from Pacaraima (MZUSP106223) has enlarged lobes that are distinctly capitate and detached from the hemipenial body, with round knobs ornamenting the lobular tips, but lack the knobs at the basis of the sulcate face. Moreover, the specimen from Pacaraima has an elongate and roughly conical hemipenial body, whereas the specimen from Abakapá-tepui has a short and globose hemipenis. Hemipenes from the populations of La Escalera and Chivatón are currently unavailable.

Discussion

The status of the Kaieteur population (*Neusticurus rudis* UCS1) is intriguing since despite a congruent morphology among all the Kaieteur specimens examined, the population is polyphyletic in our concatenated phylogeny, with two samples falling 'basal' to the rest of the eastern clade (see above and Figure 2). However, the DensiTree representation of

the species tree (Figure 2) does not detect high uncertainty in the position of *N. rudis* UCS 1 when all specimens from Kaieteur are considered a single species. Mitochondrial introgression/hybridisation may be one explanation for the polyphyletic topology observed in the population from Kaieteur National Park in our concatenated analysis.

The variation in hemipenial morphology among populations we examined is particularly striking and suggests that even low genetic divergence may separate distinct species in this group. Male genitalia have been suggested to be rapidly evolving (e.g. Eberhard 1985), and Klaczko et al. (2015) demonstrated that hemipenes evolve faster than external phenotype in *Anolis* lizards. Our results suggest that this could also be the case in *Neusticurus*, although a more comprehensive quantitative interspecific comparison is needed to corroborate this hypothesis since our sampling of hemipenes remains too limited. It is possible that further research will demonstrate that the populations we herein suggest as unconfirmed candidate species are valid species. At this stage, we believe that more data are needed, notably about possible gene flow among these populations (although hemipenial differences suggest premating isolation).

Despite these uncertainties, *Neusticurus arekuna* sp. nov. sensu stricto can be distinguished from *N. rudis* sensu stricto by morphological (mainly subtle scalation characters) and anatomical (hemipenial) features, which allowed us to take a step forward in the taxonomy of the *Neusticurus* genus.
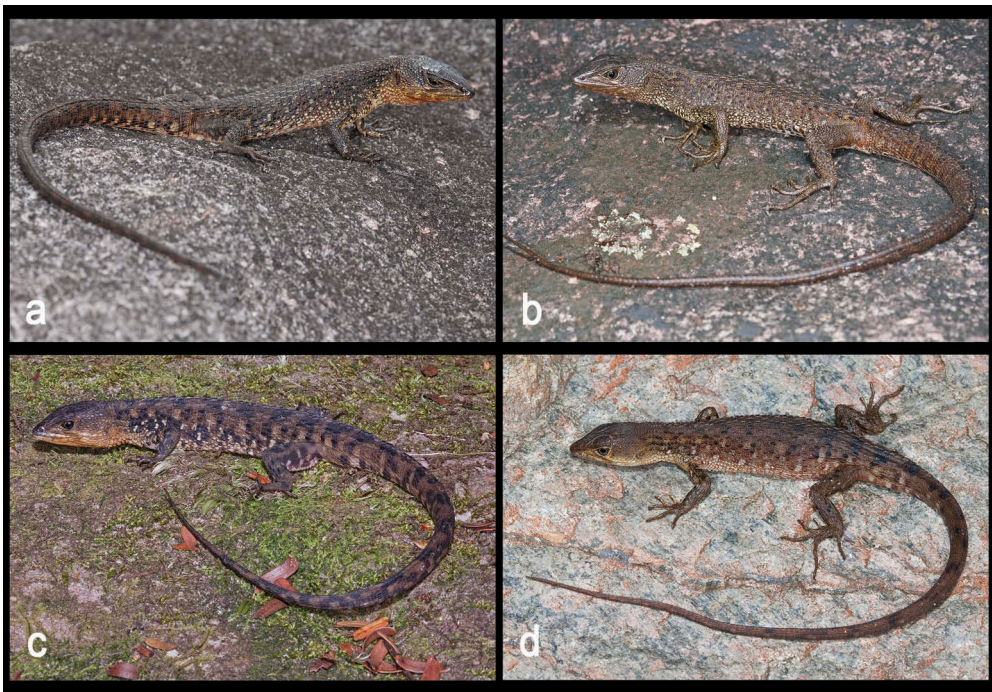
Figure 12. Variation in the *Neusticurus arekuna* clade. (a) Male *N. arekuna* UCS 1 from Abakapá-tepui, Venezuela (IRSNB18150). (b) Female *N. arekuna* UCS 3 from Auyán-tepui (IRSNB18455). (c) Male *N. arekuna* UCS 1 from Chivatón, Venezuela (IRSNB18452). (d) Female *N. arekuna* UCS 2 from La Escalera, Venezuela (IRSNB18111). Photos PJRK.

Our phylogenetic results suggest the Gran Sabana as a possible recent biogeographical barrier for *Neusticurus* in the region, which was also suggested for the frog genus *Tepuihyla* (Kok et al. 2015).

Finally, our results confirm that some taxa are ecologically plastic enough to colonise tepui summits and adapt to their peculiar climatic conditions, sometimes in drastically different habitats and much cooler climatic conditions than conspecific lowlands/uplands populations. This fits a biogeographical hypothesis for biotic diversification in Pantepui formulated by Mayr and Phelps (1967) named the Habit Shift theory. The Habit Shift theory states that some Pantepui organisms are derived from lowland ancestors/populations that shifted their habitat preference (Hoogmoed 1979; Kok 2013). Such colonisation by conspecific populations from the surrounding lowlands/uplands has not been demonstrated in many reptile taxa, especially on small topographically strongly isolated summits such as the summit of Angasima-tepui. These colonisation events highlight the complexity of diversification patterns in the area, which cannot only be attributed to vicariance or old dispersal.

Acknowledgements

Disclosure statement

Funding

References

Arévalo E, Davis SK, Sites JW Jr. 1994. Mitochondrial DNA sequence divergence and phylogenetic relationships among eight chromosome races of the *Sceloporus grammicus* complex (Phrynosomatidae) in Central Mexico. Syst Biol. 43:387–418.

Avila-Pires TCS. 1995. Lizards of Brazilian Amazonia (Reptilia: Squamata). Zool Meded. 299:1–706.

Barrio-Amorós CL, Brewer-Carías C. 2008. Herpetological results of the 2002 expedition to Sarisariñama, a tepui in Venezuelan Guayana, with the description of five new species. Zootaxa. 1942:1–68.

Bouckaert R, Heled J. 2014. DensiTree 2: seeing trees through the forest. doi:10.1101/012401

Boulenger GA. 1900. Reptiles. In: Lankester ER. II. Report on a collection made by Messrs. F. V. McConnell and J. J. Quelch at Mount Roraima in British Guiana. Trans Linn Soc Lond 2nd Ser Zool. 8(2): 53–54.

Burt CE, Burt MD. 1931. South American lizards in the collection of the American Museum of Natural History. Bull Amer Mus Nat Hist. 61:227–395.

Dixon JR, Lamar WW. 1981. A new species of microteiid Lizard (genus *Neusticurus*) from Colombia. J of Herp. 15:309–314.

Doan TM, Castoe TA. 2005. Phylogenetic taxonomy of the Cercosaurini (Squamata: Gymnophthalmidae), with new genera for species of *Neusticurus* and *Proctoporus*. Zool J Linn Soc. 403:405–416.

Donnelly MA, Myers CW. 1991. Herpetological results of the 1990 Venezuelan expedition to the summit of Cerro Guaiquinima, with new tepui reptiles. Am Mus Novit. 3017:1–56.

Dowling HG, Savage JM. 1960. A guide to the snake hemipenis: a survey of basic structure and systematic characteristics. Zoologica. 45:17–31.

Doyle AC. 1912. The lost world. London: Hodder & Stoughton; p. 319.

Drummond AJ, Suchard MA, Xie D, Rambaut A. 2012. Bayesian phylogenetics with BEAUti and the BEAST 1.7. Mol Biol Evol. 29:1969–1973.

Duméril AMC, Bibron G. 1839. Erpétologie générale, ou, Histoire naturelle complète des reptiles. Tome cinquième. Paris: Roret; p. 854.

Eberhard WG. 1985. Sexual selection and animal genitalia. Cambridge: Harvard University Press; p. 244.

Fitzinger LJ. 1826. Neue Classification der Reptilien nach ihren natürlichen Verwandtschaften : Nebsteiner Verwandtschafts-Tafel und einem Verzeichnisse der Reptilien-Sammlung des K. K. Zoologischen Museum's zu Wien. Wien: J. G. Heubner; p. 66.

Godhino R, Domingues V, Crespo EG, Ferrand N. 2006. Extensive intraspecific polymorphism detected by SSCP at the nuclear C-mos gene in the endemic Iberian lizard *Lacerta schreiberi*. Mol Ecol. 15:731–738.

Goicoechea N, Frost D, De la Riva I, Pellegrino K, Sites JW Jr., Rodrigues MT, Padial J. 2016. Molecular systematics of teioid lizards (Teioidea/Gymnophthalmoidea: Squamata) based on the analysis of 48 loci under tree-alignment and similarity alignment. Cladistics. 32:1–48.

Harvey MB, Embert D. 2008. Review of Bolivian *Dipsas* (Serpentes: Colubridae), with comments on other South American species. Herpetol Monogr. 22:54–105.

Hoogmoed MS. 1973. Notes on the herpetofauna of Surinam IV. The lizards and amphisbaenians of Surinam. Biogeographica. 4:330–346.

Hoogmoed MS. 1979. The herpetofauna of the Guianan region. In: Duellman WE, editor. The South American Herpetofauna: its origin, evolution and dispersal. Lawrence: University of Kansas. Monograph 7; p. 241–279.

Katoh K, Standley DM. 2013. MAFFT multiple sequence alignment software version 7: improvements in performance and usability. Mol Biol Evol. 30:772–780.

Klaczko J, Ingram T, Losos J. 2015. Genitals evolve faster than other traits in Anolis lizards. J Zool. 295:44–48.

Kocher TD, Thomas WK, Meyer A, Edwards SV, Pääbo S, Villablanca FX, Wilson AC. 1989. Dynamics of mitochondrial DNA evolution in animals: amplification and sequencing with conserved primers. Proc Natl Acad Sci. 86:6196–6200.

Kok PJR 2013. Islands in the Sky: Species Diversity, Evolutionary History, and Patterns of Endemism of the Pantepui Herpetofauna. [PhD thesis]. The Netherlands: Leiden University.

Kok PJR. 2015. A new species of the Pantepui endemic genus *Riolama* (Squamata: Gymnophthalmidae) from the summit of Murisipán-tepui, with the erection of a new gymnophthalmid subfamily. Zool J Linn Soc. 174:500–518.

Kok PJR, Dezfoulian R, Means DB, Fouquet A, Barrio-Amorós CL. 2018a. Amended diagnosis and new description of *Pristimantis marmoratus* (Boulenger, 1900) (Amphibia: Craugastoridae), with description of its advertisement call and notes on its breeding ecology and phylogenetic relationships. Eur J Taxon. 397:1–30.

Kok PJR, MacCulloch RD, Means DB, Roelants K, Van Bocxlaer I, Bossuyt F. 2012. Low genetic diversity in tepui summit vertebrates. Curr Biol. 22:R589–R590.

Kok PJR, Ratz S, MacCulloch RD, Lathrop A, Dezfoulian R, Aubret F, Means DB. 2018b. Historical biogeography of the palaeoendemic toad genus *Oreophrynella* (Amphibia: Bufonidae) sheds a new light on the origin of the Pantepui endemic terrestrial biota. J Biogeogr. 45:26–36.

Kok PJR, Ratz S, Tegelaar M, Aubret F, Means DB. 2015. Out of taxonomic limbo: a name for the species of *Tepuihyla* (Anura: Hylidae) from the Chimantá Massif, Pantepui region, northern South America. Salamandra. 51:283–314.

Kok PJR, Russo VG, Ratz S, Means DB, MacCulloch RD, Lathrop A, Aubret F, Bossuyt F. 2017. Evolution in the South American "Lost World": insights from multilocus phylogeography of stefanias (Anura, Hemiphractidae, *Stefania*). J Biogeogr. 44:170–181.

Lanfear R, Calcott B, Ho SY, Guindon S. 2012. PartitionFinder: combined selection of partitioning schemes and substitution models for phylogenetic analyses. Mol Biol. 29:1695–1701.

Linnaeus C. 1758. Systema Naturæ per regna tria naturæ, secundum classes, ordines, genera, species, cum characteribus, differentiis, synonymis, locis. Tomus I. Editio decima, reformata. 10th ed. Holmiæ: Laurentii Salvii; p. 824.

Maddison DR, Maddison WP. 2005. MacClade 4 v. 4.08 for OSX. Sunderland (MA): Sinauer Associates.

Mägdefrau H, Mägdefrau K. 1994. Biologie, Haltung und Zucht einer Wasserteju-Art (*Neusticurus*) vom Guaiquinima-Tafelberg, Venezuela. Herpetofauna. 16:15–20.

Mägdefrau H, Mägdefrau K, Schlüter A. 1991. Herpetologische Daten vom Guaiquinima-Tepui, Venezuela. Herpetofauna. 16:13–26.

Manzani PR, Abe AS. 1988. Sobre dois novos métodos de preparo de hemipenis de serpentes. Mem Inst Butantan. 50:15–20.

Marques-Souza S, Prates I, Fouquet A, Camacho A, Kok PJR, Nunes PMS, Dal Vechio F, Sousa Recoder R, Mejia N, Teixeira Junior M, et al. in press. Reconquering the water: evolution and systematics of South and Central American aquatic lizards (Gymnophthalmidae). Zool Scripta.

Mayr E, Phelps WS. 1967. The origin of the bird fauna of the south Venezuelan highlands. Bull Amer Mus Nat Hist. 136:269–328.

McDiarmid RW, Donnelly MA. 2005. The herpetofauna of the Guayana highlands: amphibians and reptiles of the Lost World. In: Donnelly MA, Crother BI, Guyer C, Wake MH, White ME, editors. Ecology and evolution in the tropics: a herpetological perspective. Chicago: University of Chicago Press; p. 461–560.

Müller L. 1923. Neue oder seltene Reptilien und Batrachier der Zoologischen Sammlung des bayr. Staates. Zool Anz. 58:291–297.

Myers CW, Donnelly MA. 2001. Herpetofauna of the Yutaje–corocoro massif, Venezuela: second report from the Robert G. Goelet American Museum–terramar expedition to the Northwestern tepuis. Bull Am Mus Nat Hist. 261:1–85.

Myers CW, Donnelly MA. 2008. The summit herpetofauna of Auyantepui, Venezuela: report from the Robert G. Goelet American Museum–terramar Expedition. Bull Am Mus Nat Hist. 308:1–147.

Nunes PMS, Fouquet A, Curcio FF, Kok PJR, Rodrigues MT. 2012. Cryptic species in *Iphisa elegans* Gray, 1851 (Squamata: Gymnophthalmidae) revealed by hemipenial morphology and molecular data. Zool J Linn Soc. 166:361–376.

Palumbi SR. 1996. Nucleic acids II: the polymerase chain reaction. In: Hillis DM, Moritz C, Mable BK, editors. Molecular systematics. 2nd ed. Sunderland: Sinauer Associates; p. 205–247.

Pellegrino KCM, Rodrigues MT, Yonenaga-Yassuda Y, Sites JJW. 2001. A molecular perspective on the evolution of microteiid lizards (Squamata, Gymnophthalmidae), and a new classification for the family. Biol J Linn Soc. 74:315–338.

Pesantes O. 1994. A method for preparing the hemipenis of preserved snakes. J of Herp. 28:93–95.

Rambaut A 2016. Figtree, a graphical viewer of phylogenetic trees. [accessed 2016 Dec 20]. http://tree.bio.ed.ac.uk/software/gtree.

Rambaut A, Drummond AJ 2007. Tracer v1. 5. Computer program and documentation distributed by the Authors. [accessed 2015 Apr 01]. http://tree.bio.ed.ac.uk/software.

Rambaut A, Drummond AJ. 2009. FigTree v1. 4.2. Computer program and documentation distributed by the Authors. [accessed 2015 Apr 01]. http://tree.bio.ed.ac.uk/software.

Rivas GA, Molina CR, Ugueto GN, Barros TR, Barrio-Amorós CL, Kok PJR. 2012. Reptiles of Venezuela: an updated and commented checklist. Zootaxa. 3211:1–64.

Ronquist FM, Teslenko P, van der Mark DL, Ayres A, Darling S, Höhna B, Larget L, Liu M, Suchard A, Huelsenbeck JP. 2012. MrBayes 3.2: efficient Bayesian phylogenetic inference and model choice across a large model space. Syst Biol. 61:539–542.

Roze JA. 1958. Resultados zoológicos de la expedición de la Universidad Central de Venezuela a la región del Auyantepui en la Guayana Venezolana, abril de 1956. 5. Los reptiles del Auyantepui, Venezuela, basándose en las colecciones de las expediciones de Phelps-Tate, del American Museum of Natural History, 1937–1938, y de la Universidad Central de Venezuela, 1956. Acta Biol Venez. 2:243–270.

Saint KM, Austin CC, Donnellan SC, Hutchinson MN. 1998. C-mos, a nuclear marker useful for squamate phylogenetic analysis. Mol Phylogenet Evol. 10:259–263.

Sánchez-Pacheco SJ, Torres-Carvajal O, Aguirre-Peñafiel V, Nunes PMS, Verrastro L, Rivas GA, Rodrigues MT, Grant T, Murphy RW. 2017. Phylogeny of *Riama* (Squamata: Gymnophthalmidae), impact of phenotypic evidence on molecular datasets, and the origin of the Sierra Nevada de Santa Marta endemic fauna. Cladistics. doi:10.1111/cla.12203

Savage JM. 1997. On terminology for the description of the hemipenes of squamate reptiles. Herpetol J. 7:23–25.

Swofford DL. 2002. PAUP*. Phylogenetic Analysis Using Parsimony (* and other methods). Ver. 4. b.10. Sunderland (MA): Sinauer Associates.

Torres-Carvajal O, Lobos SE, Venegas PJ, Chávez G, Aguirre-Peñafiel V, Zurita D, Echevarría LY. 2016. Phylogeny and biogeography of the most diverse clade of South American gymnophthalmid lizards (Squamata, Gymnophthalmidae, Cercosaurinae). Mol Phylogenet Evol. 99:63–75.

Tschudi JJ von. 1845. Reptilium conspectus quae in republica Peruana reperiuntur er pleraque observata vel collecta sunt in itenere. Archiv Für Naturgeschichte. 11(1):150–170.

Uetz P, Hosek J 2017. The reptile database. [accessed 2017 Jan 30]. http://www.reptile-database.org.

Uzzell TM. 1966. Teiid lizards of the genus *Neusticurus* (Reptilia, Sauria). Bull Amer Mus Nat Hist. 132:277–328.

Uzzell TM. 1973. A revision of lizards of the genus *Prionodactylus*, with a new genus for *P. leucostictus* and notes on the genus *Euspondylus* (Sauria, Teiidae). Postilla. 159:1–67.

Van Bocxlaer I, Loader SP, Roelants K, Biju SD, Menegon M, Bossuyt F. 2010. Gradual adaptation toward a range-expansion phenotype initiated the global radiation of toads. Science. 327:679–682.

Yang Z, Rannala B. 2012. Molecular phylogenetics: principles and practice. Nature Rev Genet. 13:303–314.

Zaher H. 1999. Hemipenial morphology of the South American xenodontine snakes with a proposal for a monophyletic Xenodontinae and a reappraisal of colubroid hemipenes. Bull Amer Mus Nat Hist. 240:1–168.

Appendix 1. Additional comparative material examined (not listed in Table 2).

Neusticurus bicarinatus
GUYANA. *Potaro-Siparuni*, Mabura Hill: 1 adult ♂ (MTKD D47740). Kaieteur National Park: 1 adult ♀ (IRSNB18458).

Neusticurus racenisi
BRAZIL. *Roraima*, Serra de Parima: 1 adult ♂ (MZUSP9773); 2 adult ♀♀ (MZUSP9772, MZUSP12965).

Neusticurus surinamensis
BRAZIL. *Amapá*, Serra do Navio: 2 subadult ♂♂ (MZUSP78141, MZUSP78145); 3 adult ♀♀ (MZUSP78142, MZUSP78144, MZUSP79404). Vila Nova: 1 subadult ♂ (MZUSP78140); 1 subadult [unsexed] (MZUSP78179); 1 juvenile ♂ (MZUSP78143). *Pará*, Taboleiro Leonardo, Rio Trombetas: 1 juvenile ♀ (MZUSP53813). Município de Oriximiná, Cruz Alta: 1 adult ♀ (RMNH.RENA.24516). SURINAME. *Marowijne*: 1 adult ♂ (RMNH.RENA.24510); 3 adult ♀♀ (RMNH.RENA.24488, RMNH.RENA.24496, RMNH.RENA.24511). *Sipaliwini*, Nassau Mountains: 1 adult [unsexed] (RMNH.RENA.13397). FRENCH GUIANA. *Régina*, Kaw Mountains: 2 adult ♀♀ (IRSNB18149, IRSNB18457).